

Buss
Stellan FH

Rickett et FYI

SITE-94

**CAMEO: A Model of Mass-Transport Limited
General Corrosion of Copper Canisters**

Karen J. Worgan
Michael J. Apter

December 1996

ISSN 1104-1374
ISRN SKIR--96/46--SE

SKi

STATENS KÄRNKRAFTINSPEKTION
Swedish Nuclear Power Inspectorate

SKI Report 96:46

SITE-94

**CAMEO: A Model of Mass-Transport Limited
General Corrosion of Copper Canisters**

Karen J. Worgan
Michael J. Apted

Quantisci Inc., 3900 S. Wadsworth Blvd., Suite 555,
Denver, Colorado 80235, USA

December 1996

SKI Project Number 94095

This report concerns a study which has been conducted for the Swedish Nuclear Power Inspectorate (SKI). The conclusions and viewpoints presented in the report are those of the authors and do not necessarily coincide with those of the SKI.

Norstedts Tryckeri AB
Stockholm 1998

PREFACE

This report concerns a study which is part of the SKI performance assessment project SITE-94. SITE-94 is a performance assessment of a hypothetical repository at a real site. The main objective of the project is to determine how site specific data should be assimilated into the performance assessment process and to evaluate how uncertainties inherent in site characterization will influence performance assessment results. Other important elements of SITE-94 are the development of a practical and defensible methodology for defining, constructing and analyzing scenarios, the development of approaches for treatment of uncertainties and evaluation of canister integrity. Further, crucial components of an Quality Assurance program for Performance Assessments were developed and applied, including a technique for clear documentation of the Process System, the data and the models employed in the analyses, and of the flow of information between different analyses and models.

Björn Dverstorp
Project Manager

TABLE OF CONTENTS

	Page
1. Introduction	1
2. Background	2
2.1 CALIBRE	2
2.2 CAMEO	4
3. Review of the Chemistry of Copper Corrosion	4
3.1 General Corrosion of Copper under Reducing Conditions	7
3.2 General Corrosion of Copper under Oxidizing Conditions	8
3.3 Corrosion Limited by Oxygen-Transport Rate	9
3.4 Corrosion Limited by Copper Chloride-Transport Rate	11
3.4.1 Equilibrium Solubility of Dissolved Copper Chloride	12
3.4.2 Oxidation of Cu(I) to Cu(II)	13
3.5 Kinetics of Copper Dissolution	14
3.6 Precipitation of Copper Corrosion Products	15
4. Mathematical Models	16
4.1 Copper Corrosion Controlled by Sulphide Transport to the Canister	16
4.2 Copper Corrosion Controlled by Oxygen Transport to the Canister	19
4.3 Copper Corrosion Controlled by Copper Chloride Transport away from the Canister	21
5. Numerical Methods	25
6. Scoping Calculations	26
6.1 Data Inputs	26
6.2 Corrosion Limited by Sulphide-Transport Rate	26
6.3 Corrosion Limited by Oxygen-Transport Rate	29
6.4 Corrosion Limited by Copper Chloride-Transport Rate	29
7. Future Enhancements	34
References	36

LIST OF FIGURES AND TABLES

FIGURES

	Page
Figure 2.1 Conceptual Model of the Near-Field of a Spent Fuel Repository	3
Figure 2.2 Section of the Near-Field Modelled in CALIBRE (with Spent Fuel, No Canister) and CAMEO (with Canister, No Spent Fuel)	3
Figure 3.1 Stability Relations among Copper Compounds in the System Cu-H ₂ O-O ₂ -S at 25°C and 1 Atmosphere Total Pressure, Dissolved Sulphur Species = 10 ⁻¹ m.	6
Figure 3.2 Schematic of Chemical and Transport Processes Affecting General, Uniform Corrosion of Copper Canisters under Oxidizing Conditions	10
Figure 4.1 Conceptual Model for Corrosion by Sulphide or O ₂	17
Figure 4.2 Illustration of Sulphide Concentration Profiles in the Bentonite Buffer at Various Times	19
Figure 6.1 Comparison of Oxygen Diffusion and Copper Chloride Diffusion as Rate-Determining Mechanisms for Corrosion of Copper Canisters	32

TABLES

Table 6.1 Tabulation of Parameters that Are Fixed for These Sensitivity Calculations, and Their Values and Measurement Units.	27
Table 6.2 Results of CAMEO Sensitivity Calculations for General Corrosion of Copper Canisters Controlled by Diffusive Transport of Sulphur Species.	28
Table 6.3 Results of CAMEO Sensitivity Calculations for General Corrosion of Copper Canisters Controlled by Diffusive Transport of Dissolved Oxygen	28
Table 6.4 Results of CAMEO Sensitivity Calculations for General Corrosion of Copper Canisters Controlled by Diffusive Transport of Copper Chloride	31

1. INTRODUCTION

This report describes the technical basis for the CAMEO code, which models the general, uniform corrosion of a copper canister either by transport of corrodants to the canister, or by transport of corrodant products away from the canister. The current Swedish concept for the final disposal of spent nuclear fuel is based on the KBS-3 repository concept [1], and more recently, the SKB-91 concept [2]. According to this concept, extremely long containment times ($\geq 10^6$ years) are achieved by thick (60-100 mm) copper canisters. Internal vessels of mild steel are proposed for mechanical support, but these vessels do not significantly extend the time of containment provided by the outer copper canister, and corrosion of mild steel is not further considered in this report. Each canister is surrounded by a compacted bentonite buffer, located in a saturated, crystalline rock at a depth of around 500 m below ground level.

The failure of the canister by corrosion has been considered in KBS-3 [1], SKB-91 [2] and Project-90 [3], and to occur by the general corrosion of copper with sulphides present in reducing (low Eh) groundwater. The corrosion rates are limited by the rate of transport of sulphides (present in the bentonite buffer and the groundwater of the host rock) to the canister surface, where reaction with the copper is assumed to occur instantaneously. Small, empirical pitting factors are introduced to account for the possibility of early failure by localized pitting.

Recent research by workers in Canada [4, 5] has focused on copper corrosion occurring under oxidizing conditions. Oxygen may be present initially in the repository trapped at closure. Owing to the limited supply of oxygen initially introduced by repository excavation and waste package emplacement, it is believed that the aerobic corrosion of copper by this mode will be short-lived. Oxidants may also be produced initially by the γ -radiolysis of water, but the importance of this effect is mitigated by thick canister walls and by decreasing radioactive decay over time. Deep circulation of oxygenated groundwater may also occur in some postulated scenarios. Under oxidizing conditions, general corrosion rates are assumed to be limited either by the diffusive mass-transport rate of oxygen to the canister surface or by the diffusive mass-transport rate reaction product (copper chloride) away from the canister surface.

Accordingly, three diffusive transport-limited cases are identified for general, uniform corrosion of copper:

1. General corrosion rate-limited by diffusive mass-transport of sulphide to the canister surface under reducing conditions.
2. General corrosion rate-limited by diffusive mass-transport of oxygen to the canister surface under mildly oxidizing conditions.
3. General corrosion rate-limited by diffusive mass-transport of copper chloride species away from the canister surface under highly oxidizing conditions.

The CAMEO code includes general corrosion models for each of the above three processes. CAMEO is based on the well-tested CALIBRE code [6, 7], previously developed as a finite-difference, mass-transfer analysis code for the SKI to evaluate long-term radionuclide release and transport in the near-field. This initial version of CAMEO is intended to support the specific, limited objectives of SKI's SITE-94

project, as well as provide a suitable framework for future enhancements to modelling general corrosion of copper canisters.

The organization of this report is as follows: the background to the code is given in Chapter 2; the chemistry of copper corrosion is described in Chapter 3; the mathematical models that form the basis for the code are set out in Chapter 4; the numerical methods employed in CAMEO to solve those equations are described in Chapter 5; Chapter 6 presents results from a series of scoping calculations made to evaluate sensitivity in predicted failure times of copper canisters by these various general corrosion models; and possible future enhancements to the code are discussed in Chapter 7.

2. BACKGROUND

The CAMEO code has been developed by adaptation of the CALIBRE near-field model of radionuclide transport [6, 7]. CALIBRE was originally developed to evaluate mass-transfer limited release and migration of radionuclides within the near field, for use in the Swedish Nuclear Power Inspectorate's Project-90 safety assessment of a reference repository for spent nuclear fuel [3].

2.1 CALIBRE

The conceptual model of the near field for an SKB-91 repository design is illustrated in Figure 2.1. The buffer surrounding the canister is made of compacted bentonite, and the tunnel is backfilled with a sand-bentonite mixture. The fractured rock is idealized, such that the fractures occur in the horizontal plane, are plane-parallel and are spaced at regular intervals in the vertical direction. This idealization allows the CALIBRE model to take advantage of the symmetry of such a system. The section of the canister and near field modelled in CALIBRE is illustrated in Figure 2.2.

The inner Z-axis shown in the diagram corresponds to the vertical axis of the cylindrical canister, and is represented by a zero-flux boundary condition. The upper and lower horizontal symmetry boundaries are similarly represented. At the far radial boundary, a fixed boundary concentration condition, typically assumed to be zero, is imposed.

An alternative configuration sets the concentration at the upper boundary to zero. In this option, there is an upper section of buffer above the canister, and the upper boundary represents the buffer and tunnel intersection.

As an option, the CALIBRE code can calculate the outward migration of a redox front, produced by the radiolysis of water in the canister, following failure. The canister as a barrier to transport is not modelled in CALIBRE. Instead, it is assumed to provide a specific period of complete containment, during which time only nuclide decay and ingrowth is calculated.

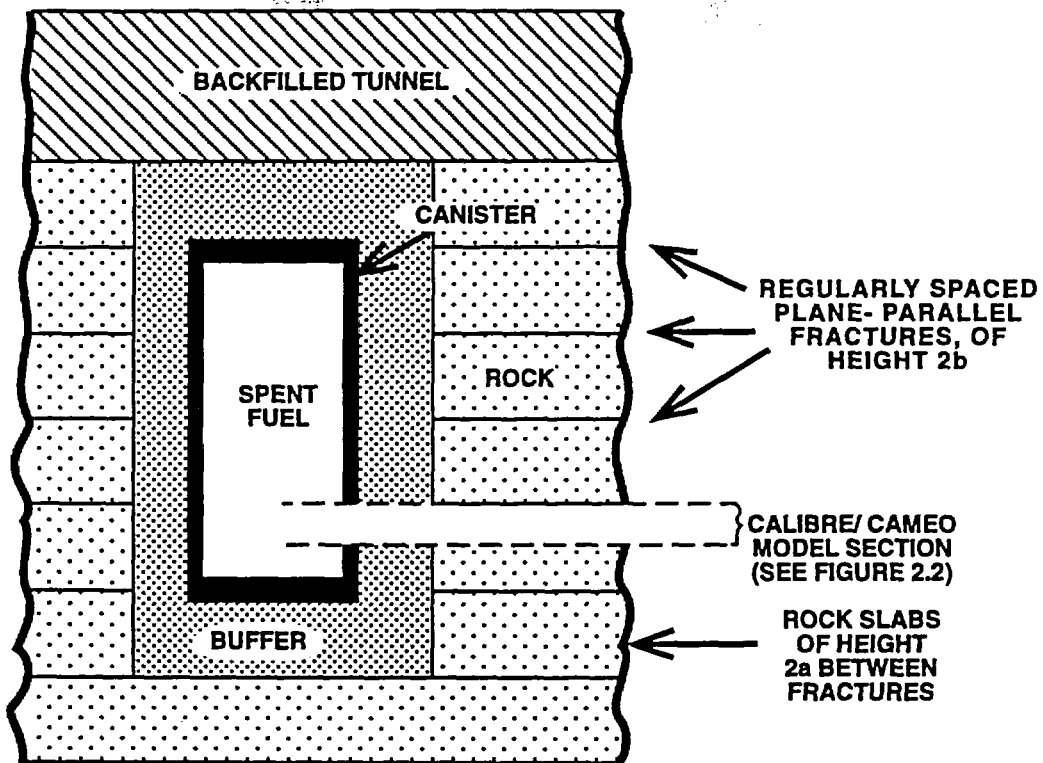


Figure 2.1 Conceptual Model of the Near-field for CAMEO.

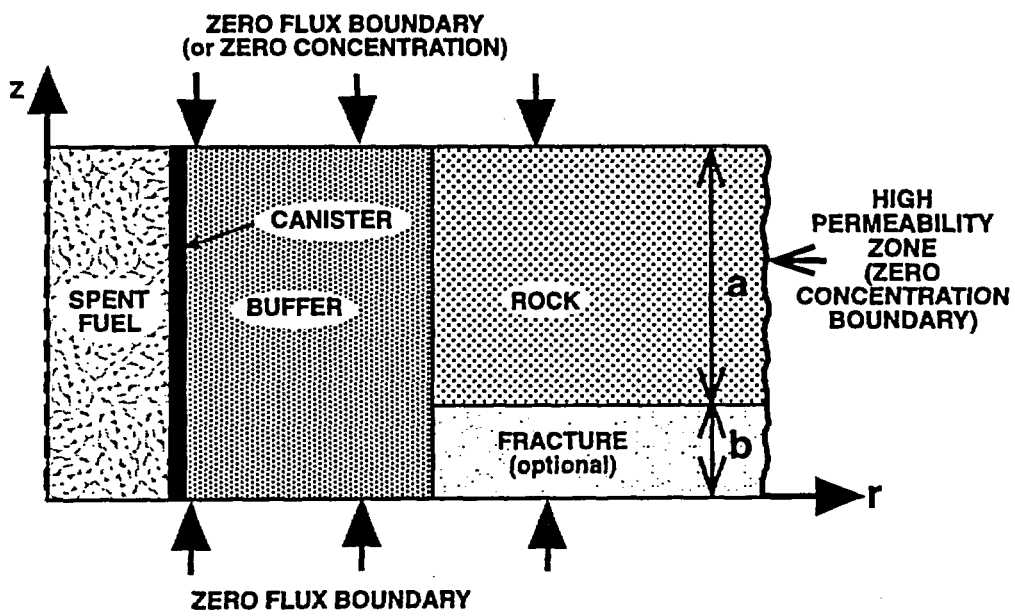


Figure 2.2 Section of the Near-field Modelled in CAMEO (Canister Included, Spent Fuel Not Included).

After container failure, the redox front motion is calculated first, if required. This is then used to determine whether oxidizing or reducing elemental solubility limits and distribution coefficients are used, at each grid cell. The code then calculates the spent fuel dissolution, and the migration of nuclides through the near-field by diffusion in the buffer and rock, and by diffusion and advection in the fracture. Advection is treated approximately, to preserve the two-dimensionality of the problem. The approximation is described in full in the CALIBRE technical report [6], together with verification tests that compare CALIBRE results with those obtained in KBS-3 [1].

Initial concentrations of radionuclides are assigned by the user, corresponding to measured levels in the host rock, which are zero for most radionuclides. Solubility limits for key radioelement-bearing solids are applied throughout the modelled region. This is necessary because of possible gradients in chemical conditions, especially arising from the redox front, where changes between oxidizing and reducing conditions may cause precipitation of radionuclide-bearing solids.

The transport equations are solved by approximating the differential equations by difference equations in time and space. Radionuclide decay and ingrowth are handled by an exact numerical formula that separates the decay calculation from the transport calculation at each timestep. Similarly, the ratio of total mass concentration to dissolved concentration for each nuclide is assumed to remain constant over a timestep, to avoid the solution of non-linear equations. Errors introduced by these approximations are minimized by employing an adaptive time-stepping algorithm. The algorithm imposes small steps during periods of rapidly changing conditions, and larger ones as the system approaches steady-state.

2.2 CAMEO

The CAMEO code uses the same geometry and numerical methods for solving the transport equations as the CALIBRE code. The major differences are in the chemical boundary conditions and dissolution model for the copper canister, when it reacts with Cl^- ions in the pore water. For the oxygen and sulphide corrodant cases, the near-field components include only the copper canister and bentonite buffer, with a constant outer concentration of these reactive species assumed at the bentonite/rock interface. For the sulphide case, uniformly distributed iron-sulphide solids can be modeled as part of the bentonite backfill that additionally contribute reactive sulphide species. The geometry of the problem is one-dimensional in the radial direction, so that the transient and steady-state results can be readily verified using an analytic model. The corrosion model diffusive transport of copper chloride away from the canister surface includes the rock and fracture, as the fracture transport can enhance the flux of copper corrodants away from the canister.

3. REVIEW OF THE CHEMISTRY OF COPPER CORROSION

Copper has been selected for a long-term canister material for two principal reasons. First, copper displays an extensive range of thermodynamic stability over likely repository conditions. Second, for chemical environmental conditions outside of this range of stability, the rate of formation of more stable copper solids can be constrained by rate of diffusive mass-transport of reactants (or products) through the compacted bentonite buffer. Diffusive transport rates are highly predictable compared to other long-term processes that may affect near-field performance. The transport

rate sets an upper limit on the rate of general, uniform corrosion of the metallic copper canister¹. Furthermore, the rates of diffusive transport of reactive species are needed for calculation of localized corrosion reactions [8]. The modelling of such localized attacks is outside the scope of this report.

A simplified Pourbaix diagram of the thermodynamically stable solid phases for the system Cu-H₂O-O₂-S at 25°C is shown in Figure 3.1 [9]. Metallic copper (Cu) is stable under mildly reducing to mildly oxidizing conditions over the expected mildly acidic to slightly alkaline (6 > pH > 10) conditions that can be expected at the copper interface with compacted bentonite buffer [10].

At more reducing conditions, copper sulphides (or copper-iron sulphides if sufficient iron is present) become more stable than metallic copper, assuming that sulphide is present. There are many possible non-stoichiometric copper sulphide phases with slightly variable compositions that can form and meta-stably persist under such reducing conditions [8].

With increasing oxidizing conditions, cuprite (Cu₂O) becomes more stable than copper. At even more oxidizing conditions, tenorite (CuO) becomes more stable than cuprite. For extremely high concentrations of dissolved chloride under mildly to strongly oxidizing conditions, various copper chloride and mixed chloride-oxyhydroxides may be more stable than the corresponding pure oxides of copper [8].

Based on these relatively simple thermodynamic relations for copper and copper compounds, three transport-control mechanisms for general corrosion of copper canisters have been identified. These are:

1. General corrosion rate-limited by diffusive mass-transport of sulphide to the canister surface under reducing conditions.
2. General corrosion rate-limited by diffusive mass-transport of oxygen to the canister surface under mildly oxidizing conditions.
3. General corrosion rate-limited by diffusive mass-transport of copper chloride species away from the canister surface under oxidizing conditions.

Both the mode and the rate of general corrosion of the copper canisters will be strongly affected by the chemical environment of the repository, and in particular, the conditions at the canister/buffer interface. Conceptual models for the chemical processes impacting these three modes of general corrosion are discussed in the following sections. In addition, a simple transition-state model is used to describe the effect of precipitation of corrosion products on the overall corrosion rate of copper.

¹ The rates of interfacial attachment or detachment reactions (i.e., corrosion kinetics) at the canister surface might, under certain circumstances, further limit the rate of general corrosion of the canister. These effects are typically disregarded, however, as unnecessary for a robust and technically defensible estimate of the mean canister lifetime.

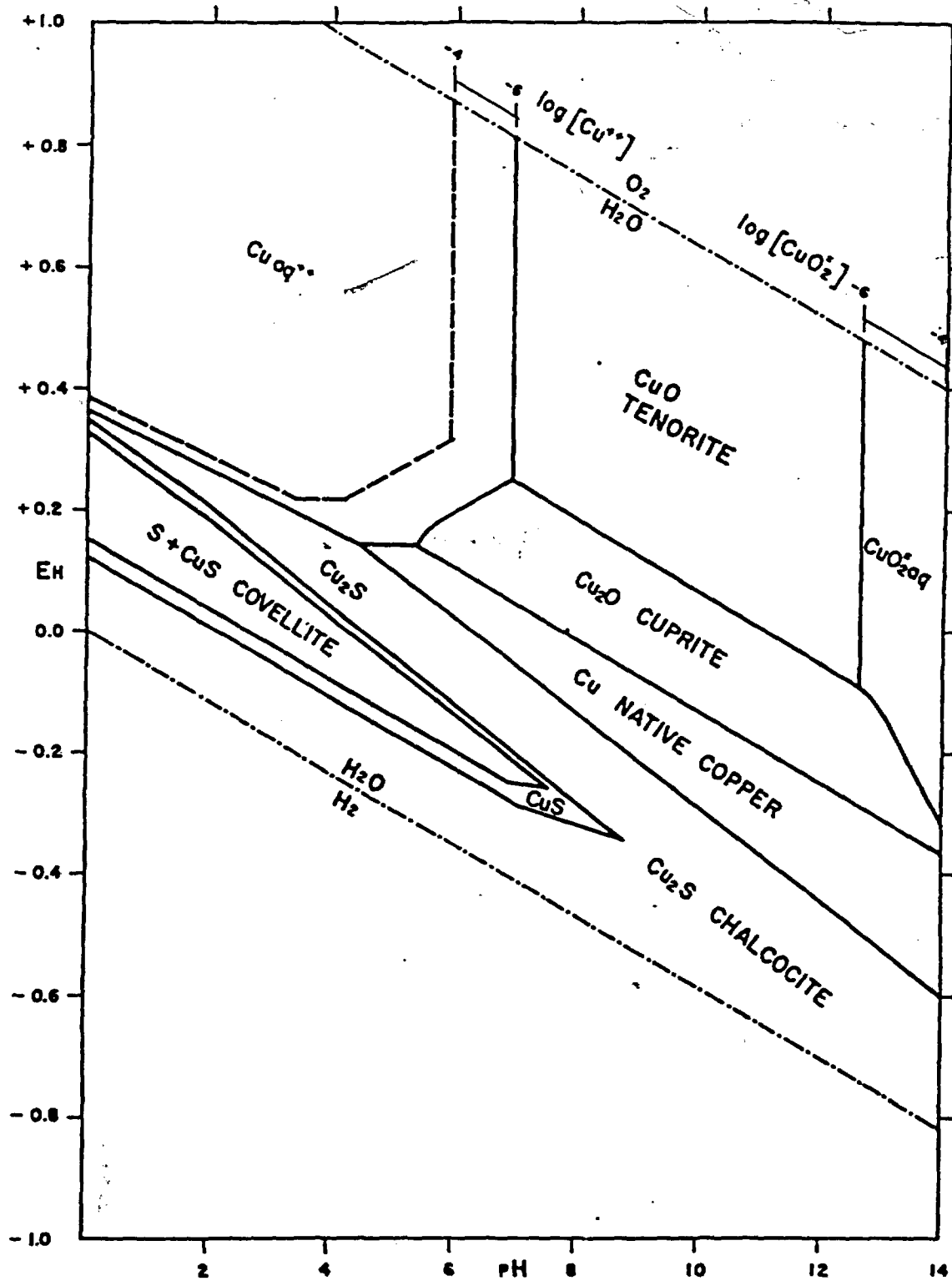


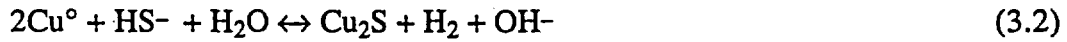
Figure 3.1 Stability Relations among Copper Compounds in the System Cu-H₂O-O₂-S at 25°C and 1 Atmosphere Total Pressure, Dissolved Sulphur Species = 10⁻¹ m (after [9]).

3.1 General Corrosion of Copper under Reducing Conditions

The mass-transport rate of dissolved sulphide (or total dissolved sulphur species) through the bentonite buffer to the canister surface is the fundamental model for evaluating the long-term general corrosion rate of copper canisters in performance analyses conducted by the SKB [1, 2]. The chemical reaction of copper metal, Cu^0 , can be written as:



or, equivalently written as:



Each mole of aqueous sulphide species² (HS^-) that arrives at the copper surface is assumed to react with two moles of copper to form chalcocite, Cu_2S . While other stoichiometric copper sulphides are possible, chalcocite conservatively represents the highest ratio of moles of copper consumed by corrosion per mole of sulphide. Instantaneous reaction is assumed, so that no credit is taken for reaction kinetics between copper and aqueous sulphide species. Nor is any credit taken for decreases in corrosion rates arising from possible passivating or protective layers that might form on the copper.

There are several potential sources of dissolved sulphide. The closest source is the disseminated iron sulphides (pyrite or pyrrhotite) that can occur as a minor phase (a few weight percent) within the bentonite. The presence of such distributed sulphides will act to locally buffer the concentration of dissolved aqueous sulphide species at the solubility value for the iron sulphide. As sulphide is consumed in the general corrosion of copper, this will cause the iron sulphides to undergo further dissolution. This will continue up to the point the iron sulphide phase is completely consumed and the local concentration of dissolved sulphide decreases to zero. Iron sulphides closest to the copper canister will be consumed first, and a depletion front for iron sulphide will sweep outwards over time until this front reaches the buffer-host rock interface. The rate of migration of this front will be controlled by the amount of iron sulphides present in the bentonite.

Also important for the long-term general corrosion rate of copper canisters is the concentration of sulphide at the buffer-rock interface. This concentration is assumed to be fixed over all time because the rate of replenishment by advective transport in the far field is expected to be significantly greater than the rate of diffusive transport of sulphide into the buffer. The actual concentration of dissolved sulphide in the far field (and hence, at the buffer-rock interface) is assumed to be controlled by the dissolution of iron sulphide minerals that occur as minor phases in the granitic host rock.

² Actual low-temperature aqueous species of sulphur may include polysulphide, thiosulfate, and sulfite, depending on the pH, Eh, and total amount of sulphur present [11]. The equilibrium and kinetic relationships among these species are quite complex [12, 13]. Because the diffusive mass-transfer model for copper corrosion does not take credit for reaction kinetics and assumes a maximum ratio of moles of copper reacted per mole of total dissolved sulphur species present, the formation and metastable persistence of multiple sulphur species can only further reduce the predicted rate of copper corrosion.

Observed concentrations of dissolved sulphide in several Swedish groundwaters ranges from <0.01 to 0.6 mg/l [14].

Dissolved sulphate and sulphate minerals in bentonite represent additional potential sources of sulphur that might become reduced and available for corrosion reaction with copper canisters. Below 200°C, the reduction of sulphate to sulphide in the absence of a catalyst is extremely slow and can be neglected even over time scales as long as millions of years [12]. Sulphide can, however, be formed by the microbiological reduction of sulphate in both groundwater and bentonite [15, 16]. Microbial reduction of sulphate could adversely affect the general corrosion of copper canisters by 1) increasing the amount of sulphides within the bentonite, and 2) increasing the concentration of sulphide at the buffer-rock interface. Note that because the concentration of dissolved sulphide at the buffer-rock interface is assumed to be fixed and controlled by the solubility of iron pyrites in the rock, microbial reduction of sulphate may not impact this chemical boundary condition.

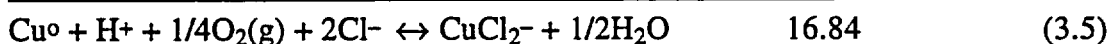
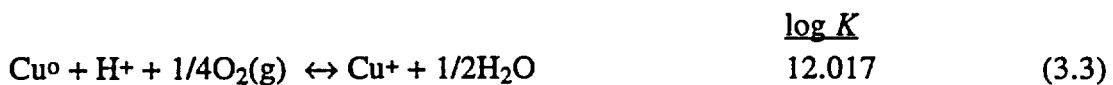
Calculations of general, uniform corrosion by these mechanisms indicate extremely long lifetimes for copper canisters (> 10⁶ years) [1, 2]. This longevity is attributable to the assumed sustained reducing conditions in deep (500-1000 meters) pores waters of granitic plutons in Sweden, and the relatively low concentration of reduced sulphur species in these waters [14]. Even when additional sources of reduced sulphur are included, such as pyrite in bentonite and microbial reduction of aqueous sulphate, the SKB estimated mean-lifetime for copper canisters is greater than 10⁶ years [17-19].

Pits may form in the canister and penetrate the canister sooner than the assumed uniform corrosion of the copper. Empirical pitting factors (i.e., the aspect ratio of the depth of pits to the depth of uniform corrosion, typically a value of 2 to 5) are applied to describe if and when a pit may lead to penetration, hence failure, of the canister.

An important assumption in this analysis is that the corrosion attack is uniform over the entire canister surface. It has been noted that, "...the corrosion attack that can occur on the copper canister will only be of importance if it has local character." [18].

3.2 General Corrosion of Copper under Oxidizing Conditions

The overall interfacial reaction (both cathodic and anodic processes) for copper dissolution under oxidizing conditions can be expressed as the summation of the following two reactions, with associated equilibrium constants K 's at 25°C [20]:



One of four processes can be expected to control the general, uniform corrosion rate of copper canisters. These are [4]:

1. transport rate of oxygen (or oxidant) to the canister surface,

2. rate of interfacial reduction of oxygen by copper,
3. rate of interfacial dissolution of copper, or
4. transport rate of dissolved copper chloride away from canister surface.

These transport rates, especially the transport rate of dissolved copper species, can be impacted by other chemical processes such as precipitation of new copper phases, oxidation of dissolved copper species ($\text{Cu(I)} \rightarrow \text{Cu(II)}$), and differential adsorption of Cu(I) and Cu(II) species on the backfill. Figure 3.2 summarizes these processes.

It has been argued that one or the other of the transport rates, steps #1 or #4, is the rate determining step for copper corrosion under oxidizing conditions [4]. Step #1 will be rate determining under mildly oxidizing (oxygen-limiting) conditions, whereas step #4 will be rate determining under highly oxidizing conditions, when the transport rate of reactants away from the corroding copper surface becomes more limiting than the rate of supply of oxygen to that surface [5]. These two transport rate-determining processes are discussed below. These models assume that the surface of the copper canister is always bare and that there is no layer of corrosion products to impede the transport of reactants to, or products from, the canister surface. Such layers, if they were to form and maintain physical cohesion, would only serve to further reduce the rate of general corrosion calculated by this model. The formation of such layers may, however, have significant effect on other, localized modes of corrosion that are outside the scope of this report. In addition to the diffusive transport-limited models, a general kinetic model for the corrosion ("dissolution") of copper is also described. While corrosion kinetics are not expected to be rate limiting, this model is included to bound the possible concentration of dissolved copper species at the canister surface; this model in CAMEO is analogous to the kinetic model for waste-form dissolution that has been well-tested in the parent CALIBRE code.

3.3 Corrosion Limited by Oxygen-Transport Rate

It is typically assumed that the rate that dissolved oxygen reaches the canister surface, R_{ox} , will be lower than the rate at which dissolved copper-chloride leaves this surface, R_{CuCl} :

$$R_{ox} \ll R_{CuCl}$$

That is to say, the *slower* of these two competing rates (oxygen-transport rate, R_{ox}) becomes the *rate limiting step* to the general corrosion rate of copper canisters. Four moles of copper will be consumed by general corrosion for each mole of dissolved oxygen that diffuses to the canister surface (see equation. 3.5).

The oxygen-transport rate through the buffer, R_{ox} , is related to gradient in the oxygen concentration (or partial pressure or fugacity) in groundwater across the buffer-rock interface. The oxygen fugacity at the canister surface is expected to be low, possibly as low as 10^{-50} bars that is required for incipient formation of cuprite, Cu_2O from copper metal [8]. This value is effectively zero for the purposes of calculating concentration gradients driving diffusion of dissolved oxygen.

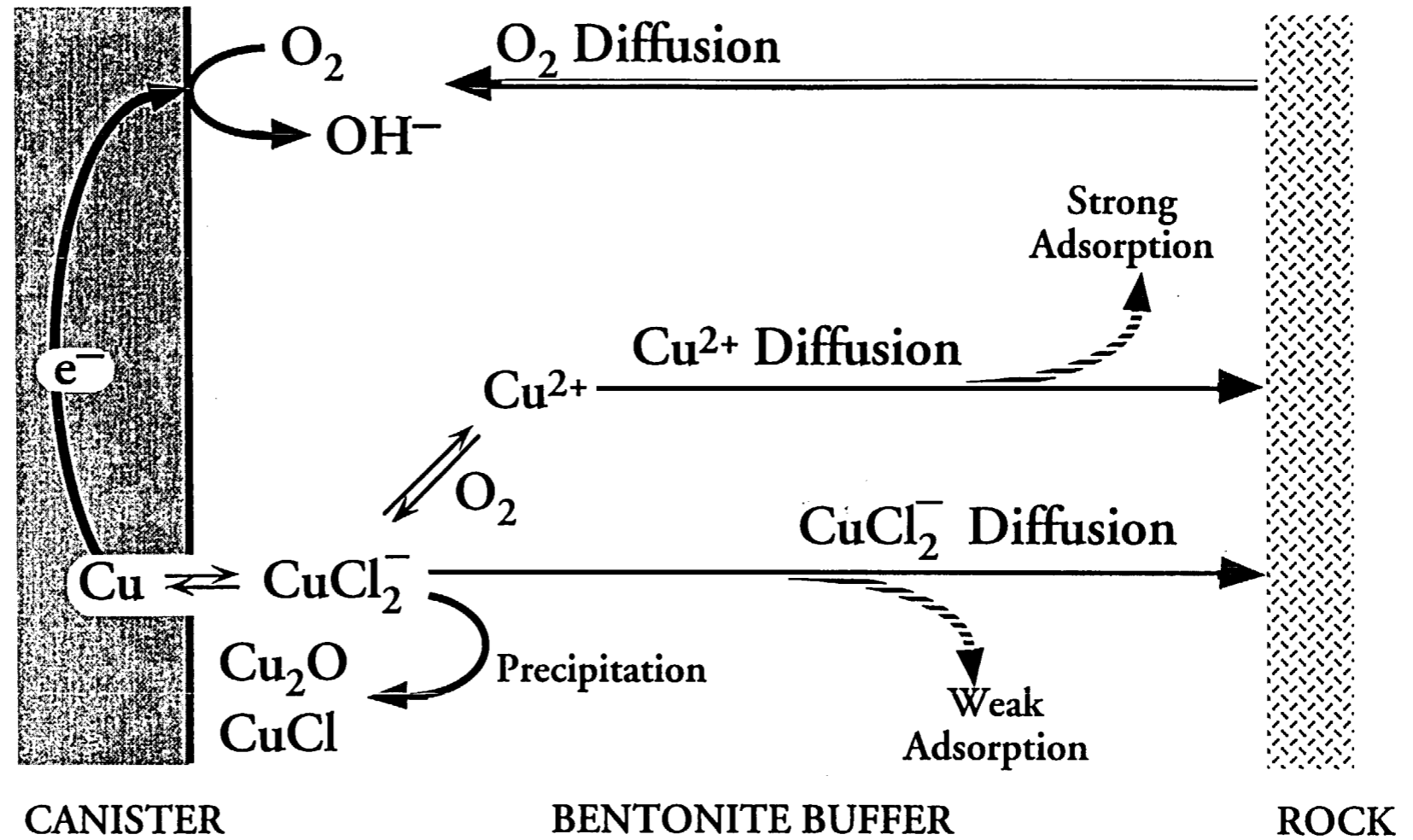


Figure 3.2 Schematic of Chemical and Transport Processes Affecting General, Uniform Corrosion of Copper Canisters under Oxidizing Conditions (after reference [5]).

Oxygen fugacities in repository groundwaters at the buffer-rock interface may be variable, ranging values approaching that for copper-cuprite equilibrium [8] and air-saturation values. With increasing oxygen fugacity at the buffer-rock interface, the rate of oxygen transport to the canister surface increases, while the rate of copper-chloride transport away from this surface remains constant. If the magnitude of increase in the oxygen-transport rate is large enough, it is possible that copper-chloride transport away from the canister surface (see section 3.4), rather than oxygen transport to the canister surface, may become the rate-limiting (i.e., slower) process in general corrosion:

$R_{ox} \gg R_{CuCl_2}$, as concentration of oxygen in repository groundwaters increases.

It is only asserted that the above relationship *may* occur; sensitivity analyses are needed to establish if, and under what conditions, the rate of oxygen-transport *may* exceed the rate of copper-chloride transport.

In CAMEO calculations, the oxygen concentration at the buffer-rock interface can be defined over a wide range by the user. Whatever value is selected, however, is considered to be time-invariant, controlled by the assumed fast advective transport of oxygen to this interface. All of the oxygen that diffuses through the buffer and reaches the canister surface is assumed to be consumed, so the inner boundary condition for the concentration of oxygen is zero. No credit is taken for the kinetics of copper corrosion by oxygen or any rate-attenuating affects arising from potentially protective or passivating layers of corrosion products, such as Cu_2O , that may form at the canister surface. CAMEO does, however, explicitly calculate the mass of Cu_2O that is formed at the canister surface, so that a time of canister failure can be predicted. The structure and assumptions for this oxygen-transport model are similar to the conceptual model for sulphide transport under reducing conditions.

Primary sources of oxygen to drive this postulated general corrosion reaction are 1) oxygen introduced and trapped in engineered materials (e.g., buffer and tunnel backfill) and rock during the construction and emplacement of the nuclear waste repository, or 2) deep circulation of oxygenated groundwater, which might arise from glaciation, changes in sea level, reactivation of faulting, etc. As with the sulphide case, the long-term, general corrosion by oxygen is determined by magnitude of the chemical concentration gradient, which is proportional to the concentration of oxygen at the buffer-rock interface.

For abundance of oxygen introduced during repository construction is limited. Estimates show that, unless this residual oxygen is somehow diverted to a limited number and/or limited surface area of emplaced canisters, the amount of copper that could be consumed by general corrosion from this source is negligible [18-19]. For deeply circulating oxygenated groundwater, it is not only the concentration of oxygen that is important but also the duration of the assumed scenario.

3.4 Corrosion Limited by Copper Chloride-Transport Rate

With increasing oxygen concentration at the buffer-rock interface, the general corrosion of copper canisters may eventually cease to be limited by the transport rate of oxygen *to* the canister surface. Instead, the general rate of corrosion may be determined by the diffusive-transport rate of reaction products, assumed to be

dissolved copper chloride (CuCl_2^-), away from the canister surface (Figure 3.2). To calculate this rate of diffusive transport of reaction products, the concentration gradient for copper chloride species (CuCl_2^-) across the buffer must be determined. The $[\text{CuCl}_2^-]$ at the buffer-rock interface is conservatively assumed to be zero (i.e., swept away boundary condition), so that the magnitude of the gradient is entirely related to the $[\text{CuCl}_2^-]$ at the canister surface.

The maximum concentration of CuCl_2^- at the canister surface is set by the equilibrium solubility of copper at the highly oxidizing redox potential assumed to be imposed at the buffer-rock interface (see next section). Note that copper metal is not the most thermodynamically stable phase under such highly oxidizing conditions (see section 3.6). Even if more stable copper-bearing phases form at the canister surface, however, the corrosion rate of the copper canister itself is assumed to be driven by the solubility of metastable copper. Other workers [5] have suggested that a mixed-potential, kinetic rate will constrain the boundary concentration for CuCl_2^- at the copper surface under such conditions; the CAMEO code can readily incorporate such an alternative constraint by the user's choice.

The net rate of transport of CuCl_2^- through buffer can be impacted by oxidation of dissolved Cu(I) to Cu(II) (Figure 3.2). Adsorption also will affect the net rate of transport, especially because anionic Cu(I) species display a much lower degree of sorption on bentonite than do cationic Cu(II) species. Moreover, CuCl_2^- may undergo redox reaction with mineral phases present in the buffer³. The impact of such additional processes on the type and concentration of dissolved copper species are described as incorporated into the CAMEO code in subsequent sections.

3.4.1 Equilibrium Solubility of Dissolved Copper Chloride

In the simplest case, the oxidation of copper metal to form CuCl_2^- at the canister surface will be constrained by the solubility of copper metal, $C_{\text{sat}}^{\text{Cu}^0}$. This can be calculated using the equilibrium constants cited previously (equation 3-5):

$$10^{16.84} = \frac{[\text{CuCl}_2^-]}{[\text{H}^+] P_{\text{O}_2}^{0.25} [\text{Cl}^-]^2} \quad (3.6)$$

$$C_{\text{sat}}^{\text{Cu}^0} = [\text{CuCl}_2^-] = 10^{16.84} [\text{H}^+] P_{\text{O}_2}^{0.25} [\text{Cl}^-]^2 \quad (3.7)$$

$$C_{\text{sat}}^{\text{Cu}^0} = 10^{16.84} 10^{-\text{pH}} P_{\text{O}_2}^{0.25} [\text{Cl}^-]^2 \quad (3.8)$$

$$C_{\text{sat}}^{\text{Cu}^0} = 10^{-4.01} 10^{16.95\text{Eh}} [\text{Cl}^-]^2 \quad (3.9)$$

³ The diffusive rate of CuCl_2^- can only become the rate-limiting step for general corrosion of copper under relatively oxidizing conditions, if at all. Thus, reducing minerals in the buffer will be contacted by ingressing dissolved oxygen, which may cause the minerals to oxidize. If such reducing minerals do not react with ingressing dissolved oxygen, then it is problematical whether these same reducing minerals would react with egressing CuCl_2^- .

where all bracketed terms are in units of moles/liter, P_{O_2} is in bars and Eh is in volts. Under certain conditions, it may be that dissolution kinetics of copper may further constrain the interfacial concentration of $CuCl_2^-$ [5]. Such kinetic constraints are discussed in section 3.5.

3.4.2 Oxidation of Cu(I) to Cu(II)

Experimental evidence indicates that the initial corrosion/dissolution of copper metal produces Cu(I) species, even under highly oxidizing conditions [5]. The conceptual model for diffusion of $CuCl_2^-$ to be the rate limiting step for general corrosion of copper requires strongly oxidizing conditions throughout the near field. It is likely for this model, therefore, that the initially released Cu(I) species will be further oxidized to Cu(II) species during transport through the buffer.

This oxidation has a significant effect of overall transport-limited corrosion of copper because the anionic Cu(I) species are only weakly adsorbed by bentonite, while cationic Cu(II) species will be strongly sorbed and retarded during transport. Strong adsorption locally decreases the dissolved concentration of copper, locally steepening the concentration gradient, hence enhancing the diffusive transport rate of copper away from the surface of the copper canister.

Sharma and Millero [21] conducted a study of copper oxidation as a function of pH, chloride, and dissolved oxygen content. They obtained the following rate expression for the rate of oxidation of Cu(I) (written as Cu^+) in solution to Cu(II):

$$\frac{d[Cu^+]}{dt} = k_{ox} [Cu^+] [O_2(aq)] \quad (3.10)$$

where [] denotes concentration in moles per kg of water and the rate constant k_{ox} in kg/mol of water/min is given by:

$$\log k_{ox} = 10.73 + 0.23 pH - \frac{2373}{T} - 3.33I^{0.5} + 1.45I \quad (3.11)$$

where T is the temperature in Kelvins and I is ionic strength in moles per kg of water. No constraints with respect to temperature, pH, chloride concentration, or ionic strength are noted by the authors.

Monovalent Na^+ is likely to be the dominant cationic species for charge neutralization with chloride. Accordingly, the ionic strength is approximated to be equal to the concentration of the chloride ion in solution, $[Cl^-]$ in moles per kg of water.

To estimate the concentration of dissolved oxygen, the equilibrium constant, K_{O_2} , for the solubility of oxygen in water is needed. This value is approximately 10^{-3} moles of O_2 per kg of water per bar of O_2 pressure [22]. For a given partial pressure of O_2 (P_{O_2} , in bars), the following relationship holds:

$$[O_2(aq)] = K_{O_2} P_{O_2} = 10^{-3} \text{ moles kg}^{-1} \text{ bar}^{-1} (P_{O_2}) \quad (3.12)$$

The relationship between P_{O_2} and Eh is:

$$\text{Eh (in volts)} = 1.23 + (0.059/4) \log P_{O_2} - 0.059\text{pH} \quad (3.13)$$

$$P_{O_2} = 10^{67.8(\text{Eh} - 1.23 + 0.059\text{pH})} \quad (3.14)$$

Combining equations 3.12 and 3.14,

$$[O_2(aq)] = 10^{-3} \text{ moles kg}^{-1} 10^{67.8(\text{Eh} - 1.23 + 0.059\text{pH})} \quad (3.15)$$

It must be cautioned that the rate law from reference [21] is derived for highly oxidizing solutions in which molecular oxygen is actually present. Under conditions that are less oxidizing, molecular oxygen may not be present as a measurable specie, which could affect the actual molecular mechanism that is implicitly assumed in the derivation within reference [21]. Unfortunately, other laboratory studies on oxidation of dissolved copper are also conducted in relatively oxidizing solutions [23].

3.5 Kinetics of Copper Dissolution

The equilibrium CuCl_2^- concentration can be assumed to be attained instantaneously, or the time-dependent approach to this value can be specifically modelled. The long-term corrosion rate of copper metal, $d(t)$, is equated to the rate of change in CuCl_2^- concentration at the canister surface. This rate of change in CuCl_2^- concentration is expressed in a transition-state formulation related to the equilibrium solubility of copper metal, $C_{\text{sat}}^{\text{Cu}}$, and the initial forward rate of dissolution (corrosion), k_+ , as:

$$d(t) = \frac{d[\text{CuCl}_2^-]}{dt} = k_+ \left(1 - \frac{[\text{CuCl}_2^-]}{C_{\text{sat}}^{\text{Cu}}}\right) \quad (3.16)$$

$$d(t) = \frac{d[\text{CuCl}_2^-]}{dt} \rightarrow k_+ \text{ as } [\text{CuCl}_2^-] \rightarrow 0 \quad (3.17)$$

$$d(t) = \frac{d[\text{CuCl}_2^-]}{dt} \rightarrow 0 \text{ as } [\text{CuCl}_2^-] \rightarrow C_{\text{sat}}^{\text{Cu}} \quad (3.18)$$

If the transport rate of CuCl_2^- is fast relative to the initial corrosion rate of copper, k_+ , the concentration of CuCl_2^- never appreciably increases at the canister surface, and the long-term corrosion rate remain approximately at a constant value of k_+ (equation 3-17). If, as is possible within a low permeability buffer, the diffusive transport rate is slow relative to initial corrosion rate, the concentration of CuCl_2^- will increase and approach the equilibrium solubility of copper, $C_{\text{sat}}^{\text{Cu}}$ (equation 3-18). Under these

latter conditions, the long-term corrosion rate becomes extremely low, equal to the rate of diffusive mass transport of CuCl_2^- away from the canister surface.

3.6 Precipitation of Copper Corrosion Products

Copper metal is unstable with respect to many other copper compounds under oxidizing conditions, and it is possible that continued copper corrosion will lead to precipitation of these more stable copper-bearing phases. For example, even relatively low partial pressures of oxygen ($\sim 10^{-50}$ bars) are sufficient to favor the precipitation of more stable (i.e., lower solubility than copper metal) cuprite, Cu_2O , from solution, where:

$$C_{sat}^{\text{Cu}^0} > C_{sat}^{\text{Cu}_2\text{O}} \text{ for } P_{\text{O}_2} > 10^{-50} \text{ bars} \quad (3.19)$$

In certain aerated tests, copper chlorides have been observed as products from corrosion of copper metal, usually forming on top of a layer of Cu_2O [5].

The effect of precipitating a new, more stable copper-bearing phase can be incorporated into the rate equation for copper corrosion. Assuming that Cu_2O is the precipitating phase with a solubility $C_{\text{Cu}_2\text{O},\text{sat}}$, the limiting rate equation for copper corrosion becomes:

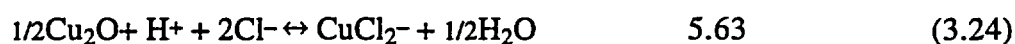
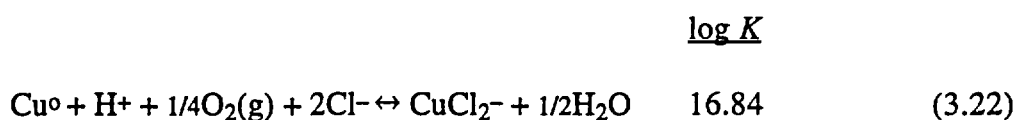
$$d(t) = \frac{d[\text{CuCl}_2^-]}{dt} = k_+ \left(1 - \frac{C_{\text{Cu}_2\text{O}}}{C_{\text{Cu}^0}} \right) \quad (3.20)$$

If the transport rate is slow relative to the initial corrosion rate of copper, the interfacial concentration of CuCl_2^- will increase, and the subsequent corrosion rate will decrease. But instead of the concentration approaching the solubility for copper metal (hence the corrosion rate approaching zero), precipitation of more stable cuprite will fix the CuCl_2^- concentration, thereby fixing a non-zero corrosion rate for copper.

$$d(t) = \frac{d[\text{CuCl}_2^-]}{dt} = k_+ \left(1 - \frac{C_{\text{Cu}_2\text{O}}}{C_{\text{Cu}^0}} \right) > 0, t \rightarrow \infty \quad (3.21)$$

Thus, precipitation of cuprite (or any other copper-bearing solid) at the canister interface maintains an elevated rate of copper corrosion compared to the non-precipitation case.

The solubility of cuprite, $\text{Cu}_2\text{O}(s)$ ($C_{\text{Cu}_2\text{O},\text{sat}}$, in units of moles/liter) can be derived from the equilibrium rate constants, K [20]:



$$10^{5.63} = \frac{[\text{CuCl}_2^-]}{[\text{H}^+][\text{Cl}^-]^2} \quad (3.25)$$

$$C_{\text{sat}}^{\text{Cu}_2\text{O}} = [\text{CuCl}_2^-] = 10^{5.63} [\text{H}^+][\text{Cl}^-]^2 \quad (3.26)$$

$$C_{\text{sat}}^{\text{Cu}_2\text{O}} = 10^{5.63 - \text{pH}} [\text{Cl}^-]^2 \quad (3.27)$$

where all bracketed terms are in units of moles/liter.

4. MATHEMATICAL MODELS

The following section describe how the conceptual models previously identified are mathematically modelled for inclusion in the CAMEO code.

4.1 Copper Corrosion Controlled By Sulphide Transport to the Canister

The conceptual model for transport of dissolved sulphides or oxygen is illustrated in Figure 4.1. Radial geometry is used in this model (r = distance from the package center), so that it may be solved analytically, by the use of a quasi-stationary approximation [24, 25].

The initial pore-water concentration of sulphide (or oxygen) in the buffer is uniform, with a value ranging from zero up to the solubility limit of the sulphide species (or oxygen) considered. The bentonite may contain minor amounts of iron sulphides that are conservatively assumed to readily dissolve to produce aqueous sulphide, if the pore-water concentration falls below the solubility limit for this phase. In reality, the dissolution of pyrite may entail formation of dissolved sulphide, as well as other sulphur species such as polysulphides, thiosulfate, etc. CAMEO solves a moving-boundary problem, $R(t)$, where R is the radial position of the boundary between saturated and unsaturated sulphide conditions. The mass conservation equation is given by:

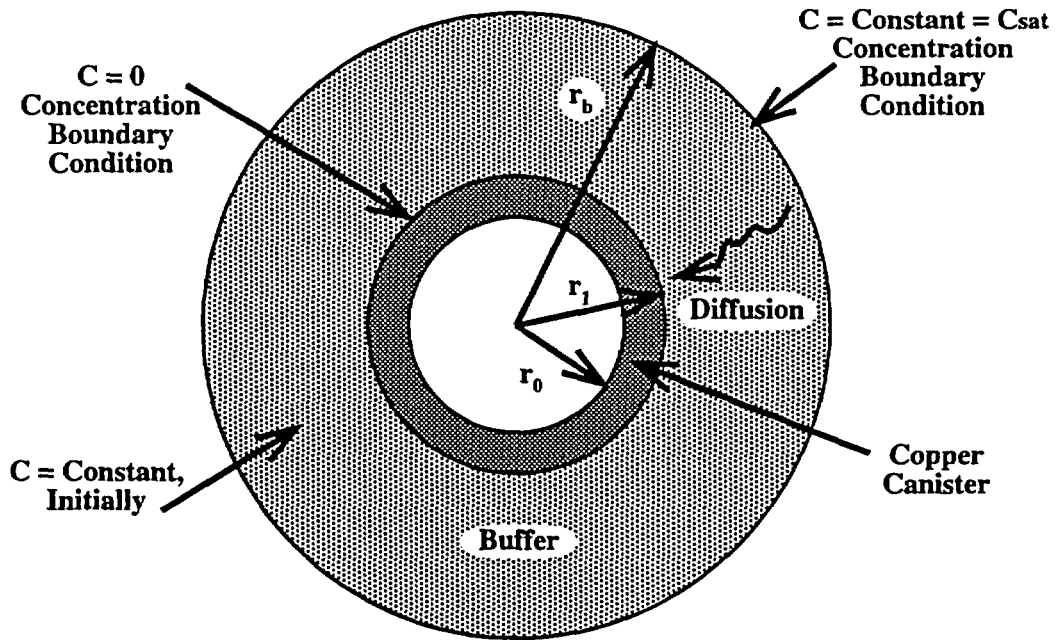


Figure 4.1 Conceptual Model for Corrosion by Sulphide or O₂

$$\phi_B \frac{\partial C(r,t)}{\partial t} = \frac{D_B}{r} \frac{\partial \{r \frac{\partial C(r,t)}{\partial r}\}}{\partial r} \quad (4.1)$$

where ϕ_B is the porosity of the buffer, $C(r,t)$ is the concentration of sulphide, and D_B is the effective diffusion coefficient of the buffer. The boundary conditions are given by:

$$C(r_1) = 0 \quad (4.2)$$

$$C(R(t)) = C_{sat}^{Fe-S} \quad (4.3)$$

where r_1 is the canister radius and C_{sat}^{Fe-S} is the solubility limit of iron sulphide.

The flux at the moving boundary is given by the front velocity, $dR(t)/dt$, multiplied by the undissolved mass concentration:

$$D_B \frac{\partial C(R(t),t)}{\partial r} = \frac{dR(t)(A_o - \phi_B C_{sat}^{Fe-S})}{dt} \quad (4.4)$$

where A_o is the total mass concentration of material in the buffer that can be converted to sulphide, plus the dissolved concentration. For simplicity in the model, the sulphide in the solid in the buffer is considered to be of the same species as that of the dissolved concentration (i.e. effectively it is treated as a precipitate of that species). When the local dissolved concentration falls as a result of diffusion, the precipitate is assumed to pass into solution instantaneously, attempting to bring the local concentration of HS^- back up to the solubility of the solid iron sulphide. By assuming that all of the sulphur from the iron sulphide dissolves as HS^- , the maximum concentration gradient for this reactant is imposed, thereby assuring that a conservative maximum diffusive flux of HS^- to the canister is maintained. Once all the iron sulphide at a given location has dissolved, the boundary position advances outward. This process continues until the moving boundary reaches the outer radius of the buffer.

The quasi-stationary approximation assumes a solution of the following form for the concentration in the buffer at a radial position r , between the inner boundary and outer, moving boundary:

$$C(r,t) = \frac{C_{sat}^{Fe-S}}{\ln(R(t)/r_1)} (\ln r - \ln r_1) \quad (4.5)$$

Differentiating (4.5) with respect to r and substituting $\partial C/\partial r$ at $r = R(t)$ into equation (4.4) gives the following differential equation for $R(t)$:

$$R \frac{dR}{dt} \ln \frac{R}{r_1} = \frac{D_B C_{sat}^{Fe-S}}{A_o - \phi_B C_{sat}^{Fe-S}} \quad (4.6)$$

This can be integrated to give a relationship between R and t :

$$R^2 \ln \frac{R}{r_1} + \frac{1}{2}(r_1^2 - R^2) = \frac{2D_B C_{sat}^{Fe-S} t}{A_o - \phi_B C_{sat}^{Fe-S}} \quad (4.7)$$

The flux $F(t)$ at the canister surface, $r = r_1$ is calculated from equations (4.4) and (4.6):

$$F(t) = \frac{D_B C_{sat}^{Fe-S} S}{r_1 \ln(R(t)/r_1)} \quad (4.8)$$

where S is the surface area of the canister. The analytic solution can be compared with that obtained using the CAMEO code, and provides a verification test case for the numerical model of precipitation employed in the code.

When the moving boundary arrives at the outer boundary of the buffer, the concentration profile in the buffer remains constant, together with the flux of corrodants consumed at the canister. The concentration profile and flux are defined by equations (4.12) and (4.13) in the next section, where C_s is the solubility limit of

the iron sulphide.

CAMEO tracks the total consumption of copper by the sulphide corrodants. Each mole of dissolved sulphide (S^{2-}) is assumed to consume 2 moles of copper. The code outputs time series of both the flux of sulphide at the canister surface and the thickness of copper left, due to uniform corrosion, as well as pitting corrosion, using empirical pitting factors. The profile concentrations in the buffer at various times are illustrated in Figure 4.2.

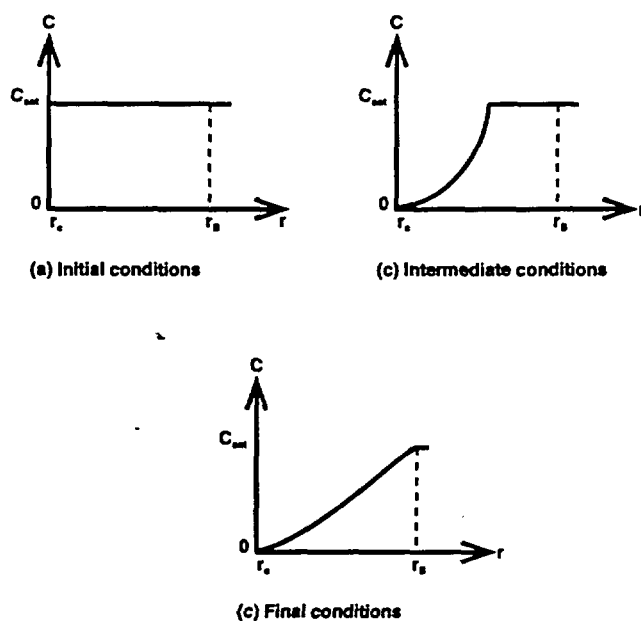


Figure 4.2 Illustration of Sulphide Concentration Profiles in the Bentonite Buffer at Various Times.

4.2 Copper Corrosion Controlled by Oxygen Transport to the Canister

The initial concentration of dissolved oxygen in the buffer is assumed to be constant, at a value specified by the user. The concentration of oxygen in the groundwater at the outer radius of the bentonite is maintained at the solubility limit of oxygen at all times. This constitutes a conservative assumption. The O_2 initially in pore waters of bentonite could help maintain this maximum value for a period of time, dependent on the amount of this residual oxygen. Alternatively, it is possible that this maximum value may be externally controlled by postulated deep circulation of oxygenated groundwater. The supply of O_2 may be limited in these scenarios, however, and so O_2 would be depleted over time.

The oxygen is transported to the canister by diffusion, with no sorption in the buffer. At the copper canister, all the oxygen is assumed to be consumed instantaneously. The actual O_2 concentration may be controlled by formation of a redox buffering couple, defined by copper metal and some $Cu(I)$ corrosion product (e.g., Cu_2O).

This buffered O_2 concentration is so low ($P_{O_2} \approx 10^{-50}$ bars) that it is effectively zero for these calculations.

The equation of mass conservation of oxygen in the buffer is given by:

$$\phi_B \frac{\partial C(r,t)}{\partial t} = \frac{D_B}{r} \frac{\partial \{r \frac{\partial C(r,t)}{\partial r}\}}{\partial r} \quad (4.9)$$

where D_B is the effective diffusion coefficient in the buffer, ϕ_B is its porosity and $C(r,t)$ is the oxygen concentration. The boundary conditions are given by:

$$C(r=r_1) = 0 \quad (4.10)$$

$$C(r=r_B) = C_{sat}^{O_2} \quad (4.11)$$

where r_1 is the outer radius of the canister, r_B is the outer radius of the bentonite buffer, and $C_{sat}^{O_2}$ is the dissolved oxygen concentration at the outer boundary.

Initially, the oxygen concentration profile across the buffer will change, decreasing from the fixed $C_{sat}^{O_2}$ value at the buffer rock interface toward the canister. Eventually the concentration profile will reach a steady state, given by:

$$C(r) = C_{sat}^{O_2} \frac{\ln(r/r_B)}{\ln(r_B/r_1)} \quad (4.12)$$

The flux of oxygen at the canister surface, $F(r_1)$ will also be constant, defined by:

$$F(r_1) = -\frac{D_B C_{sat}^{O_2}}{r_B \ln(r_B/r_1)} \quad (4.13)$$

In the model, the inward displacement of the copper canister surface by corrosion is neglected, with respect to transport. Each mole of oxygen arriving at the canister surface is assumed to consume four moles of copper, uniformly across the entire canister surface. CAMEO tracks the number of moles of copper left in the canister. At specified output times, CAMEO converts the mass of copper left into an equivalent canister thickness. The outer radius of the canister at time t , $r(t)$ is given by:

$$r(t) = \sqrt{\left(r_1^2 - \frac{4N(t)M_{Cu}}{L\rho\pi} \right)} \quad (4.14)$$

where $N(t)$ is the total number of moles of oxygen consumed by the copper at time t , M_{Cu} is the molecular weight of copper, ρ is the density of copper and L is the canister length. Note that the relatively small area represented by the ends of the canister are not accounted for in this model.

The thickness of the canister at time t is then simply $r(t) - r_o$. A pitting factor P is also applied, to determine the thickness, T , left after pitting corrosion. At time t , this is:

$$T = r_1 - r_o - P[r_1 - r(t)] \quad (4.15)$$

4.3 Copper Corrosion Controlled by Copper Chloride Transport from the Canister

The corrosion of copper by chloride ions in mildly oxidizing groundwater has been described in Chapter 3. The full model involves a number of interacting, or coupled processes. In this first version of CAMEO, a simpler model has been implemented that contains the essential features of the more complex model.

The code calculates the dissolution of the copper canister in a manner that is analogous to the dissolution of spent fuel in the CALIBRE code. Similarly, the conversion of Cu (I) species to Cu(II) species is conceptually analogous to radionuclide decay and ingrowth of a parent nuclide to a stable daughter.

Let M_o be the initial number of moles of Cu^o in the canister walls. In a closed system, the rate of Cu^o dissolution is defined here as (see equations 3-16 to 3-18):

$$d(t) = \frac{d[\text{CuCl}_2^-]}{dt} = k_+ \left(1 - \frac{[\text{CuCl}_2^-]}{C_{\text{sat}}^{\text{Cu}^o}}\right) \quad (4.16)$$

$$d(t) = \frac{d[\text{CuCl}_2^-]}{dt} \rightarrow k_+ \text{ as } [\text{CuCl}_2^-] \rightarrow 0 \quad (4.17)$$

$$d(t) = \frac{d[\text{CuCl}_2^-]}{dt} \rightarrow 0 \text{ as } [\text{CuCl}_2^-] \rightarrow C_{\text{sat}}^{\text{Cu}^o} \quad (4.18)$$

$d(t)$ is the dissolution (i.e., corrosion) rate in units of mass/unit area/unit time, k_+ is a forward reaction rate, and $[\text{CuCl}_2^-]$ is the concentration of CuCl_2^- ions in solution. $C_{\text{sat}}^{\text{Cu}^o}$ is the solubility limit of Cu^o at user-defined values of groundwater Eh, pH and CT concentration. Under closed-system, sufficiently low Eh conditions, the concentration of CuCl_2^- may reach $C_{\text{sat}}^{\text{Cu}^o}$ when net dissolution would cease.

Under mildly oxidizing chemical conditions, Cu_2O may be more thermodynamically stable than copper metal and it may nucleate and grow. In such cases, the concentration of CuCl_2^- will be limited by the solubility limit of Cu_2O , rather than by Cu^o . If the solubility limit of Cu_2O is less than that of Cu^o under the specified Eh, pH and CT conditions, the time-invariant minimum corrosion rate that can occur in a closed system is:

$$d(t) = \frac{d[\text{CuCl}_2^-]}{dt} = k_+ \left(1 - \frac{C_{\text{sat}}^{\text{Cu}_2\text{O}}}{C_{\text{sat}}^{\text{Cu}^o}}\right) > 0, t \rightarrow \infty \quad (4.19)$$

where $C_{Cu_2O_{sat}}$ is the solubility limit of Cu_2O at the specified Eh, pH and CI values.

In the CAMEO code, the copper chloride ions are released to the buffer region immediately adjacent to the copper canister. The rate of release is given by:

$$\frac{dM(t)}{dt} = -d(t)S(t) \quad (4.20)$$

where $M(t)$ is the mass of copper remaining at time t , $d(t)$ is defined by equation (4.16) and $S(t)$ is the canister surface area at time t :

$$S(t) = 2\pi LR(t) \quad (4.21)$$

$R(t)$ is the outer radius of the canister surface, and may be expressed in terms of the mass of copper at time t :

$$R^2(t) = r_1^2 - \frac{M(t)M_{Cu}}{\pi\rho L} \quad (4.22)$$

In the near-field system considered in CAMEO, the copper is assumed to dissolve in a pore water volume V , in the region immediately adjacent to the canister surface. In this region, the equation for mass conservation for Cu(I) species is given by:

$$\frac{\partial A^{Cu^+}}{\partial t}(r, z, t) = \frac{1}{V} \frac{dM(t)}{dt} + \frac{D_B}{r} \frac{\partial}{\partial r} \left(r \frac{\partial C^{Cu^+}}{\partial r} \right) + \frac{D_B \partial^2 C^{Cu^+}}{\partial z^2} - KC^{Cu^+} \quad (4.23)$$

A^{Cu^+} is the total concentration of Cu(I) species, defined by:

$$A^{Cu^+} = (\phi_B + \rho_B K_B^{Cu^+}) \quad (4.24)$$

where $K^{Cu^+}_B$ is the equilibrium distribution coefficient for Cu(I) in the buffer, while ϕ_B and ρ_B are the bentonite porosity and density, respectively.

The constant K in equation (4.23) represents the mass rate of reaction (conversion) of Cu(I) species to Cu(II) species, in solution. K is determined by groundwater Eh and pH, according to the equation:

$$K = k_{ox}[O_2(aq)] \quad (4.25)$$

where k_{ox} and $[O_2(aq)]$ are defined as in Section 3. K defines the rate of conversion of Cu(I) in solution to Cu(II), in the following way:

$$\frac{dC^{Cu^+}}{dt} = -KC^{Cu^+} \quad (4.26)$$

$$\frac{dC^{Cu^{2+}}}{dt} = KC^{Cu^+} \quad (4.27)$$

If the constant K is large enough, the majority of Cu(I) will be converted to Cu(II) at each timestep, which will drive the forward rate of copper metal corrosion to its maximum rate. Away from the dissolution region, the mass conservation for Cu(I) species is identical to that given in equation (4.23), but without the source term $(1/V)(dM/dt)$.

The mass conservation of Cu(II) species in the buffer is given by:

$$\frac{\partial A^{Cu^{2+}}}{\partial t}(r, z, t) = \frac{D_B}{r} \frac{\partial}{\partial r} \left(r \frac{\partial C^{Cu^{2+}}}{\partial r} \right) + \frac{D_B}{\partial z^2} C^{Cu^{2+}} + KC^{Cu^+} \quad (4.28)$$

The total concentration of Cu(II) species is defined by

$$A^{Cu^{2+}} = C^{Cu^{2+}} (\phi_B + \rho_B K_B^{Cu^{2+}}) \quad (4.29)$$

where $K^{Cu^{2+}_B}$ is the bentonite distribution coefficient for Cu(II).

At the innermost boundary of the model, (i.e. at the canister/bentonite interface), and at the upper and lower boundaries, conditions of zero flux are imposed:

$$D_x \frac{\partial C^i}{\partial r}(r = r_1) = 0 \quad (4.30)$$

$$D_x \frac{\partial C^i}{\partial z}(z = 0) = 0 \quad (4.31)$$

$$D_x \frac{\partial C^i}{\partial z}(z = Z) = 0 \quad (4.32)$$

where superscript i denotes either of the Cu(I) or Cu(II) species, subscript x denotes either the bentonite, rock or fracture medium and Z represents the value of the z -coordinate at the uppermost boundary of the model.

Similar mass conservation equations apply in the rock for both species, but different values are used for the diffusion coefficient, D_R , porosity, ϕ_B , density, ρ_B and distribution coefficients, $K^{Cu^+_B}$ and $K^{Cu^{2+}_B}$. At the interface between the bentonite and rock (at $r = r_B$), flux continuity is imposed:

$$-D_{B-R} \frac{\partial C^i_B}{\partial r}(r_B, z, t) = -D_{B-R} \frac{\partial C^i_R}{\partial r}(r_B, z, t), \quad b < z < Z \quad (4.33)$$

where D_{B-F} is the diffusion coefficient across the bentonite/rock interface, b is the half-width of the fracture (Figure 1.2) and subscripts B and R denote bentonite and rock, respectively. In CAMEO, the interface diffusion coefficient is defined as a weighted average of the bentonite and rock diffusion coefficients. The weights are determined by the volumes of the finite difference cells on either side of the interface, divided by the sum of their volumes.

At the bentonite/fracture interface, continuity of flux is similarly imposed:

$$-D_{B-F} \frac{\partial C_B^i}{\partial r} = -D_{B-F} \frac{\partial C_F^i}{\partial r}, \quad 0 < z < b \quad (4.34)$$

Subscript F denotes the fracture, and D_{B-F} is the interface diffusion coefficient calculated from a weighted average of the bentonite and fracture diffusion coefficients.

Flux continuity is also imposed at the horizontal interface of the rock and fracture. The boundary condition may be written:

$$-D_{R F_s} \frac{\partial C_R^i}{\partial z}(r, b, t) = -D_{R F_s} \frac{\partial C_F^i}{\partial z}(r, b, t) \quad (4.35)$$

The rock diffusion coefficient is used as the interface diffusion coefficient, in this case, as it controls the transfer rate across the interface. F_s is the fraction of the fracture surface available for rock-matrix diffusion. It may be expressed in terms of the specific wet surface area, a , the fracture half-width, b and the fractured rock porosity, θ :

$$F_s = \frac{ab}{\theta} \quad (4.36)$$

The flux term in equation (4.35) is calculated using a channel connection-length parameter to determine the average separation distance between channels in the fracture, and between channels and the rock matrix. This length is used, instead of the actual physical distance between the rock and fracture finite-difference cells, when calculating the transfer flux between rock and fracture. This parameter is used to obtain a response to the effects of channeling that is more consistent with far-field codes such as CRYSTAL [3], than can be gained by use of the specific wet surface area parameter alone. The concept behind the channel connection length is that a few large channels in the fracture will have a greater separation distance than many smaller channels that are more densely packed, even if the channel surface areas are the same. Hence, the opportunity for matrix diffusion is less, in the former case. Similarly, in the code, the larger the channel connection-length used to determine the flux between fracture and rock matrix, the lower the concentration gradient and rock matrix diffusion. This is discussed in more detail in the CALIBRE technical report [6].

The far radial boundary condition in the rock and an optional fracture is given by:

$$C^i(r_R, z, t) = 0 \quad (4.37)$$

where r_R is the radius of the outer boundary, in the rock and fracture. In the fracture, transport of either Cu(I) or Cu(II) in the radial direction is supplemented by an advection term. Mass conservation in the fracture is given by:

$$\frac{\partial A^i}{\partial t}(r, z, t) = \frac{D_F}{r} \frac{\partial}{\partial r} \left(r \frac{\partial C^i}{\partial r} \right) + \frac{F_s D_R}{\partial z^2} C^i \pm K C^i + v \frac{\partial}{\partial t} \left\{ \left(1 - \frac{r_B^2}{r^2} \right) (\beta_o - \beta_i) C^i(r, z, t) \right\} \quad (4.38)$$

β_o, β_i are weighting functions, used to average the concentration at a given radial position in the fracture, over the third, angular dimension. v is the velocity of water in the fracture, far from the deposition hole. Full details of the advective term are given in the CALIBRE technical report [6].

5. NUMERICAL METHODS

The model equations set out in the previous chapter are solved by discretizing them in both space and time. The spatial discretization is constrained such that the inner boundary formed by the first column of cells coincides with the outer boundary of the intact copper canister, in the cases of sulphide or O_2 corrodants. In the case of copper dissolution and copper-chloride transport, the innermost column of cells represents the bentonite next to the canister. The canister itself is not modelled explicitly, but is represented instead by the corrosion model. Cell boundaries are also constrained to coincide with the bentonite/rock, bentonite/fracture and fracture/rock interfaces. An optional fracture is represented by a single row of cells, whose widths are equal to half the fracture aperture.

The time component is discretized using a fully-implicit scheme. Both the accuracy and timestep size are controlled using a step-doubling adaptive stepsize algorithm. For each timestep, the solution is calculated three times: once using the full timestep, and twice, using successive half-steps. The results using the full timestep are then compared with that obtained via the two half-steps. If the overall maximum relative error is less than a prescribed value, then the step is accepted and the timestep is increased. Otherwise, the step is repeated using successively smaller steps, until the required accuracy is obtained.

Within each timestep, the copper dissolution and conversion of Cu(I) to Cu(II) (if applicable) is decoupled from the transport. The calculations performed at each step are:

- calculate the ratio of total concentration to dissolved concentration for each species. This ratio is held fixed over the timestep, and takes account of any precipitate that may be present;
- calculate the copper dissolution (if applicable) using equations (4.16)-(4.22);
- adjust the amounts of Cu(I) in the innermost column of cells, by the dissolution amounts;
- adjust the amounts of Cu(I) and Cu(II) in solution in each cell throughout the grid. These amounts will depend on the timestep size, as defined by the discretized versions of equation (4.26) and (4.27);

- calculate the new concentrations throughout the grid, as a result of transport over the timestep period;
- for oxygen or sulphide corrodants, calculate the amount of copper lost by corrosion, equivalent to the mass of corrodant lost at the zero concentration inner boundary;
- for Cu(I) and Cu(II) transport, calculate the flux of corrodants lost at the outer boundary;
- check accuracy and adjust the timestep.

The matrix of difference equations are solved using a banded matrix solver, with bandwidth determined by the number of grid cells in the vertical, or z-direction.

Full details of the input data parameters required to run the three corrosion models, preparation of input data files and code execution will be given in the CAMEO User's Guide, in preparation.

6. SCOPING CALCULATIONS

A series of scoping calculations for the general, uniform corrosion of a reference [19] ACP copper canister are presented, using the CAMEO code. Calculations are made for the three primary diffusive mass-transport limited mechanisms. Reference data from SKI, SKB, and other sources are used, where available. The data specifications and results of these calculations are summarized in the following sections.

6.1 Data Inputs

Table 6.1 summarizes the input values for the calculational Cases presented in this report. These data are common inputs to all of the calculations for general corrosion of copper canisters; data specific to each of the three limiting mechanisms are described in the separate sections below.

6.2 Corrosion Limited by Sulphide-Transport Rate

Sensitivity calculations are reported on the rate of general corrosion of copper canisters arising from diffusion-limited mass transport of sulphur species through a compacted bentonite buffer. The assumed solubility limit for iron sulphide, $3.12 \times 10^{-2} \text{ mol/m}^3$ taken from [3], compares favorably with maximum values of dissolved bi-sulphide of about $3.4 \times 10^{-2} \text{ mol/m}^3$ measured for deep groundwaters in Swedish granites [26]. The assumed maximum sum of dissolved bi-sulphide and sulphate used in these calculations (20.8 mol/m^3) is, however, somewhat higher than the maximum sum of these species (about 9 mol/m^3) measured at a site such as Äspö [26].

Four Cases for corrosion are considered. For Case S-1, diffusion of dissolved bi-sulphide (HS^-) controlled by an assumed fixed solubility limit of iron sulphide in the

host rock. Case S-2 the same as Case S-1, with the additional consideration of iron sulphide grains distributed uniformly throughout the buffer (148 moles of iron sulphide per cubic meter of buffer). Such grains are assumed to locally impose a solubility-limited concentration for bi-sulphide until each iron sulphide grain completely dissolves. Thus, a front of sulphide depletion sweeps outward from the canister over time until Case S-2 devolves into Case S-1. Case S-3 is the same as Case S-1, except that the fixed concentration of reactive sulphide at the host rock-buffer interface is assumed to equal the sum of all dissolved sulphur species (i.e., bi-sulphide and sulphate) in the groundwater. Finally, Case S-4 is a combination of Cases S-2 and S-3. As noted previously, the formation of polysulphides, thiosulphates, and other possible sulphur species are conservatively bounded by consideration of the limiting solution species bi-sulphide and sulphate.

Table 6.1 Tabulation of Parameters that Are Fixed for Sensitivity Calculations, and Their Values and Measurement Units.

Parameter	Value	Units
Canister Thickness	0.06	m (meters)
Canister Radius (r_I)	0.4	m
Buffer Radius (r_B)	0.75	m
Buffer Thickness ($r_B - r_I$)	0.35	m
Number of Cells across Buffer	9	dimensionless
Buffer Diffusion Coefficient (D_B)	1.3×10^{-3}	m^2/year
Buffer Porosity (ϕ_B)	0.35	dimensionless
Buffer Density (ρ_B)	2050	kg/m^3
Temperature (T)	30	$^{\circ}\text{C}$
Initial Dissolution Rate of Cu (k^+)	7.7×10^{-4}	m/year
Mass of Canister	9.8×10^3	moles
Pitting Factor (P)	5	dimensionless

The results of these three calculations are presented in Table 6.2. For Case S-1, assuming a limiting bi-sulphide solubility at the host rock-buffer boundary, the calculated steady-state corrosion rate is about 4×10^{-4} mol/year. The predicted time for failure by general corrosion is 24.3 million years, which decreases to a time of 5.2 million years if an empirical pitting factor of 5 is considered⁴.

⁴ The times for canister failure do not scale linearly with pitting factor. The cylindrical shape of the canister means that the exposed surface area and remaining unreacted mass of copper change at different rates during general corrosion.

Table 6.2 Results of CAMEO Sensitivity Calculations for General Corrosion of Copper Canisters Controlled by Diffusive Transport of Sulphur Species.

Case Number	Assumed Reactive Sulphur Species*	Concentration at Rock-Buffer Interface (mol/m ³)	Iron Sulphide in Buffer	Steady-State Corrosion Rate (mol/year)	Failure Time for General Corrosion (Years)	Failure Time for Pitting Corrosion (Years)
S-1	HS-	3.12 x 10 ⁻²	No	4 x 10 ⁻⁴	24.3 x 10 ⁶	5.2 x 10 ⁶
S-2	HS-	3.12 x 10 ⁻²	Yes	4 x 10 ⁻⁴	24.3 x 10 ⁶	5.2 x 10 ⁶
S-3	HS-, SO ₄ ²⁻	20.8	No	2.7 x 10 ⁻¹	36,400	7,770
S-4	HS-, SO ₄ ²⁻	20.8	Yes	2.7 x 10 ⁻¹	36,400	7,770

* The actual dissolved aqueous species of sulphur may be considerably more complicated than these assumed, limiting species.

Table 6.3 Results of CAMEO Sensitivity Calculations for General Corrosion of Copper Canisters Controlled by Diffusive Transport of Dissolved Oxygen.

Case Number	Concentration at Rock-Buffer Interface (mol/m ³)	Steady-State Corrosion Rate (mol/year)	Failure Time for General Corrosion (Years)	Failure Time for Pitting Corrosion (Years)
O-1	5 x 10 ⁻¹	1.29 x 10 ⁻²	760,000	160,000
O-2	5 x 10 ⁻⁴	1.29 x 10 ⁻⁵	7.6 x 10 ⁸	1.6 x 10 ⁸
O-3	5 x 10 ⁻⁷	1.29 x 10 ⁻⁸	» 10 ⁹	» 10 ⁹

Inclusion of iron sulphides distributed within the buffer (Case S-2) does not significantly diminish the time for failure by either general corrosion or by pitting. This assumes that there are no additional mechanisms for localized attack arising from the presence of these distributed grains. The much larger total concentration of sulphur species assumed to be reactive in Case S-3 leads to a faster steady-state corrosion rate (2.7×10^{-1} mol/year), hence to shorter times for predicted failure by general corrosion (36,400 years) and pitting (7,770 years). This result is expected because the long-term, steady-state corrosion rate for a copper canister will be proportional to the concentration gradient of reactive sulphur species across the buffer. Again note that the potential contribution from iron sulphides distributed within the buffer (Case S-4) is negligible with respect to predicted times of failure.

6.3 Corrosion Limited by Oxygen-Transport Rate

Three Cases are considered for the general corrosion of copper canisters limited by the diffusive transport of dissolved oxygen through the buffer. Case O-1 assumes a fixed concentration of oxygen of 0.5 mol/m^3 at the host rock-buffer interface. Cases O-2 and O-3 assume fixed concentrations of $5 \times 10^{-4} \text{ mol/m}^3$ and $5 \times 10^{-7} \text{ mol/m}^3$, respectively. In all Cases the water in the pores of the buffer are assumed to be initially at the same concentration as fixed at the rock-buffer interface. By comparison, the concentration of oxygen under 1 atmosphere air-saturation is 0.63 mol/m^3 , whereas the measured concentration in relatively oxidizing granitic groundwaters found in the Canadian Shield are about 100 times lower than this [5].

Table 6.3 summarizes the results from these sensitivity calculations. The steady-state corrosion rates scale directly with oxygen concentration, decreasing from $1.29 \times 10^{-2} \text{ mol/y}$ for Case O-1 to $1.29 \times 10^{-8} \text{ mol/y}$ for Case O-3. The predicted times for failure by general corrosion and pitting corrosion are inversely proportional to the fixed oxygen concentrations. For the highest concentration, Case O-1, the predicted times are 760,000 years for general corrosion and 160,000 years for pitting corrosion (with an assumed pitting factor of 5).

Note that the rates of general corrosion by oxygen diffusion are *not* dependent on other chemical factors such as Eh or total concentration of chloride. This contrasts strongly with the results of the next section that addresses general corrosion controlled by diffusion of dissolved copper chloride (CuCl_2^-).

6.4 Corrosion Limited by Copper Chloride-Transport Rate

Under the most highly oxidizing conditions, it may be that the general corrosion rate of copper canisters becomes limited by the transport rate of copper chloride (CuCl_2^-) away from the canister surface. The exact conditions at which control of general corrosion rate crosses over from one of O_2 diffusion inward to CuCl_2^- diffusion outward must be determined through sensitivity and bounding analyses. Furthermore, there are a large number of chemical processes that affect the formation, stability and transport of CuCl_2^- through the buffer, adding to the number of sensitivity calculations. Table 6.4 summarizes all of the results.

In an effort to evaluate the overlapping effects of these different processes, the

approach taken here is to selectively and sequentially "switch-on" these different processes. The following sub-sections are divided into:

- 1) the concentration of CuCl_2^- at the canister surface controlled by copper metal solubility,
- 2) the effect of a kinetic model for dissolution of copper metal,
- 3) the effect of oxidation of CuCl_2^- in solution to Cu^{2+} , and
- 4) the effect of a 1-cm aperture fracture in the buffer.

All sensitivity calculations are performed at 30°C and the pH is assumed to be buffered at a value equal to 9 by reaction with the clay buffer [10]. The Eh values (vs. SHE) cited are assumed to be fixed and apply across the entire buffer.

6.4.1 Copper Metal Solubility Constraint

In this simplest of the conceptual models for control of copper corrosion by CuCl_2^- diffusion, the only constraint is that the concentration at the canister surface is set by the stable or meta-stable equilibrium solubility for copper metal. No effects from precipitation of corrosion products or oxidation of Cu(I) to Cu(II) is included. The solubility of copper metal is treated as a function of pH, Eh, and chloride concentration [8, 9; also see equation 3.6]. Four Cases are calculated here. Case C-1 assumes an Eh equal to 0.4V and a chloride concentration $[\text{Cl}^-]$ of 10^1 mol/m^3 . Case C-2 assumes an Eh equal to 0.0V and $[\text{Cl}^-]$ equal to 10^{-1} mol/m^3 , Case C-3 assumes Eh equal to 0.0V and $[\text{Cl}^-]$ equal to 10^1 mol/m^3 , and Case C-4 assumes an Eh equal to 0.0V and $[\text{Cl}^-]$ equal to 10^3 mol/m^3 . By comparison, representative groundwaters adopted by the SKI consider $[\text{Cl}^-]$ ranging between 0.5 and 1330 mol/m^3 [27], and a representative brine from the Canadian Shield has $[\text{Cl}^-]$ equal to 170 mol/m^3 [5].

Table 6.4 lists the predicted corrosion rates and times to failure for these Cases. Corrosion rate increase with increasing Eh and $[\text{Cl}^-]$. Comparison of Cases C-2, C-3 and C-4 confirms that the corrosion rate increases as the square of the increase in $[\text{Cl}^-]$ (see equation 3.6), while the time to canister failure decreases as the square of $[\text{Cl}^-]$.

Figure 6.1 compares these predicted corrosion rates for control by diffusive transport of CuCl_2^- versus predicted corrosion rates for control by diffusive transport of O_2 , Cases O-1 and O-3. Note that the corrosion rates controlled by CuCl_2^- diffusion are specifically calculated for different Eh values at the canister surface ranging from 0.0V (equivalent to an oxygen partial pressure of about 10^{-50} bars[8]) to 0.4V (equivalent to an oxygen partial pressure of about 10^{-20} bars[8]). In contrast, the corrosion rates controlled by O_2 diffusion assume that the concentration of dissolved oxygen at the surface of the canister is zero. Incorporating these extremely low partial pressures, however, would not appreciably change the predicted corrosion rates controlled by O_2 diffusion.

Table 6.4 Results of CAMEO Sensitivity Calculations for General Corrosion of Copper Canisters Controlled by Diffusive Transport of Copper Chloride.

Case Number	Eh (V) at Canister Surface	[Cl ⁻] (mol/m ³)	Processes Included*	Steady-State Corrosion Rate (mol/year)	Failure Time for General Corrosion (Years)	Failure Time for Pitting Corrosion (Years)
C-1	0.4	10	S	3.7 x 10 ⁻¹	2.7 x 10 ⁴	5.7 x 10 ³
C-2	0.0	0.1	S	6.1 x 10 ⁻¹²	» 10 ⁹	» 10 ⁹
C-3	0.0	10	S	6.1 x 10 ⁻⁸	» 10 ⁹	» 10 ⁹
C-4	0.0	1000	S	6.1 x 10 ⁻⁴	1.6 x 10 ⁷	3.4 x 10 ⁶
C-5	0.4	1000	KP	1.36 x 10 ⁻⁴ †	7.2 x 10 ⁷	1.5 x 10 ⁷
C-6	0.4	10	KP	1.36 x 10 ⁻⁴ †	7.2 x 10 ⁷	1.5 x 10 ⁷
C-7	0.0	1000	KC	1.1 x 10 ⁻⁴	8.9 x 10 ⁷	1.9 x 10 ⁷
C-8	0.0	10	KC	6 x 10 ⁻⁶	» 10 ⁹	» 10 ⁹
C-9	0.4	1000	KP, O	1.36 x 10 ⁻⁴ †	7.2 x 10 ⁷	1.5 x 10 ⁷
C-10	0.0	10	KC, O	6 x 10 ⁻⁶	» 10 ⁹	» 10 ⁹
C-11	0.0	1000	S, F	1.1 x 10 ⁻³	8.9 x 10 ⁶	1.9 x 10 ⁶

* S = canister surface concentration of CuCl₂⁻ constrained by copper solubility;
 KC = canister surface concentration of CuCl₂⁻ further constrained by kinetic rate law based on copper solubility;
 KP = canister surface concentration of CuCl₂⁻ further constrained by kinetic rate law based on cuprite solubility;
 O = canister surface concentration of CuCl₂⁻ impacted by oxidation of Cu(I) to Cu(II);
 F = fractured buffer configuration (see text).

† Maximum corrosion rate for KP kinetic model.

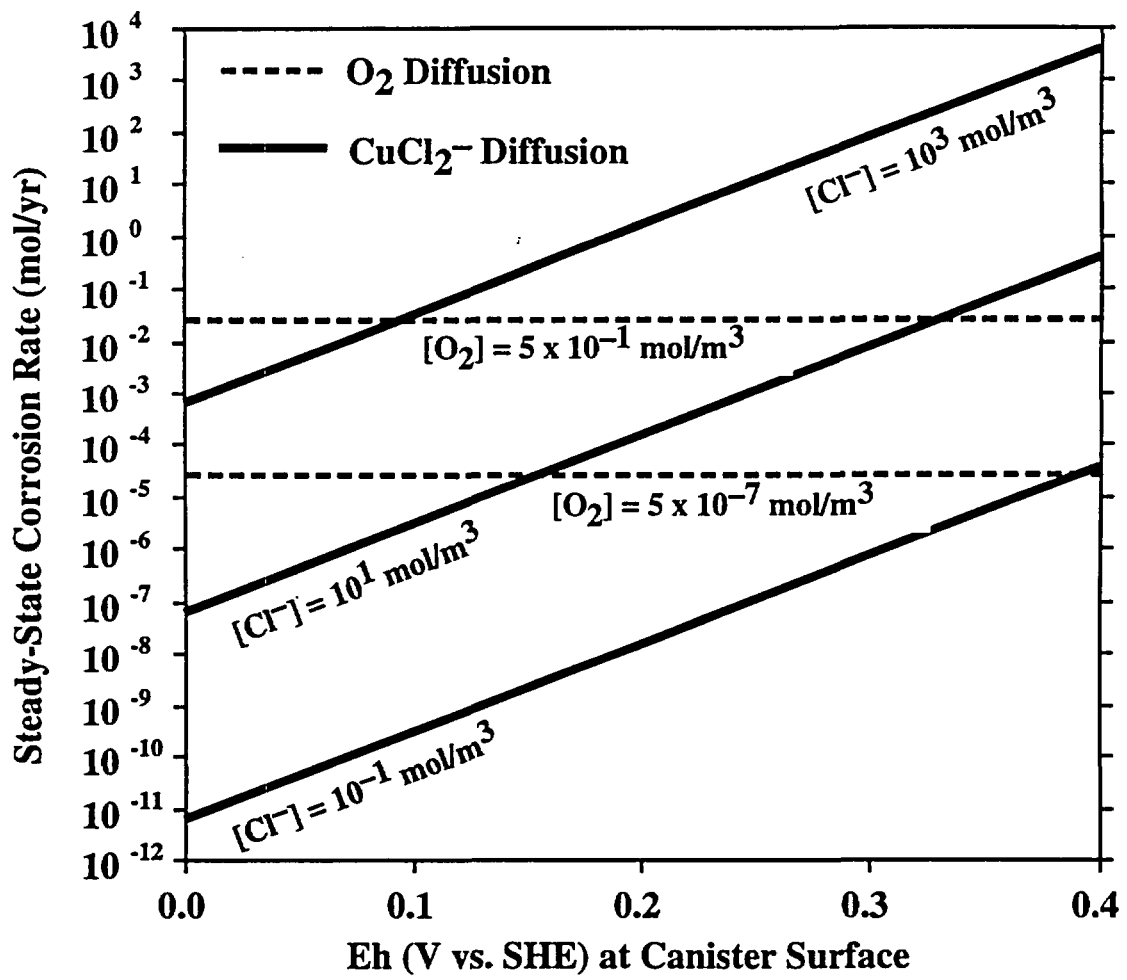


Figure 6.1 Comparison of Oxygen Diffusion and Copper Chloride Diffusion as Rate-Determining Mechanisms for Corrosion of Copper Canisters.

By comparing the predicted rates of corrosion in Figure 6.1 it can be determined under which conditions either the O₂ diffusion or CuCl₂⁻ diffusion mechanisms are controlling the corrosion rate. When the predicted rate for one mechanism is below that of the rate for the competitive mechanism, then the former mechanism is rate controlling, for that specific set of conditions. For example, Figure 6.1 shows if the O₂ concentration at the buffer-rock interface is 0.5 mol/m³ and the [Cl⁻] is equal to 10³ mol/m³, then O₂ diffusion is predicted to be the rate limiting mechanism for general corrosion down to an Eh value of 0.1V at the canister surface. Below this Eh value and for the specified groundwater chemistry, CuCl₂⁻ diffusion is predicted to control the general corrosion rate of copper. Note that increasing the O₂ concentration at the buffer-rock interface (i.e., moving from the lowest to the highest horizontal lines on Figure 6.1) extends the range of conditions under which the general rate of corrosion is controlled by CuCl₂⁻ diffusion.

6.4.2 Kinetic Model Constraint

The concentration of CuCl₂⁻ at the canister surface may be expected to be controlled by a mixed-potential, electrochemical kinetic constraint, rather than an equilibrium solubility constraint [4, 5]. This is analogous, within the context of the CALIBRE parent code to CAMEO, to the release of a radionuclide as constrained by the dissolution rate of the waste form. Instead of adopting the mixed-potential equations cited in [5] or a user-defined piece-wise-linear rate approach as in CALIBRE, we have implemented a simple transition-state conceptual model for expressing the change in corrosion rate as a function of the solubilities of copper (see equation 3.16) or cuprite (see equation 3.20) that are, in turn, functions of Eh, pH, and [Cl⁻]. Note that potential conversion of Cu(I) to Cu(II) species in solution is not incorporated into these calculations, but is incorporated into the calculations of the next section.

Four calculations are made for this conceptual model. Case C-5 assumes an Eh equal to 0.4V and a chloride concentration [Cl⁻] of 10³ mol/m³. Case C-6 assumes an Eh equal to 0.4V and [Cl⁻] equal to 10¹ mol/m³, Case C-7 assumes Eh equal to 0.0V and Cl⁻ equal to 10³ mol/m³, and Case C-8 assumes an Eh equal to 0.0V and [Cl⁻] equal to 10¹ mol/m³. Only at an Eh equal to 0.0V (and the specified pH of 9) is copper predicted to have lower solubility than cuprite. At higher Eh values, cuprite solubility is calculated to be lower; that is, cuprite is more stable than copper metal [8].

The results of these calculations are shown in Table 6.4. For the high Eh Cases (i.e., for those conditions with the highest calculated solubilities of cuprite), the corrosion rates are predicted to be equal to the maximum forward rate of reaction, k_+ in equation 3.16. Under such conditions the solubility of cuprite is much lower than the predicted (meta-stable) solubility for copper, so that from equation 3.20:

$$\frac{d[\text{CuCl}_2^-]}{dt} = k_+ \left(1 - \frac{C_{\text{sat}}^{\text{Cu}_2\text{O}}}{C_{\text{sat}}^{\text{Cu}^\circ}}\right) \rightarrow k_+, \text{ if } C_{\text{sat}}^{\text{Cu}_2\text{O}} \ll C_{\text{sat}}^{\text{Cu}^\circ} \quad (6.1)$$

For Eh = 0.0V, the predicted corrosion rates are slightly attenuated from the maximum forward rate k_+ . Note that the predicted corrosion rates for these four Cases are all lower, by many orders of magnitude under the Eh equal 0.4V conditions, than

the corrosion rates predicted for identical conditions in Cases C-1 to C-4. These latter Cases assumed no constraining kinetic model, confirming that it is conservative to ignore such kinetic model constraints in developing bounding predictions for the lifetimes of copper canisters.

6.4.3 Effect of Oxidation of Cu(I) to Cu(II) in Groundwater

Calculational Cases C-9 and C-10 are made that are identical to Cases C-5 (0.4V and a chloride concentration $[Cl^-]$ of 10^3 mol/m³) and C-8 (0.0V and a chloride concentration $[Cl^-]$ of 10^1 mol/m³), respectively, with the inclusion of a kinetic model for the oxidation of Cu(I) to Cu(II). The rate of this oxidation is a function of Eh, pH, and $[Cl^-]$ (see equation 3.10). These results are summarized in Table 6.4. The oxidation rate of Cu(I) to Cu(II) is predicted to be extremely slow, Cu(I) having an effectively infinite oxidation half life. There is no effect on the predicted corrosion rates of copper when this oxidation is included. Only for extremely high Eh conditions is the oxidation half-life of Cu(I) short enough to have any potential impact. For example, at an Eh value of 0.6V, the half-life is approximately 5.6 years. The impact of this oxidation rate on the corrosion rate of the copper canister is mitigated, however, by the fact that the corrosion rate is controlled at the initial forward rate (k_+) under such highly oxidizing conditions.

6.4.4 Effect of Fractured Buffer

A unique feature of the CALIBRE/CAMEO codes is the ability to analyze the effect of fractures/fissures having different transport characteristics than the media that they traverse. To demonstrate this capability with CAMEO, Case C-11 is calculated, identical to Case C-4 (Eh equal to 0.0V and $[Cl^-]$ equal to 10^3 mol/m³), with the inclusion of an assumed fractured buffer with a 1-m spacing between fractures and a fracture aperture of 0.01 m. The predicted general corrosion rate for Case C-11, reported in Table 6.4, is approximately twice as high as that predicted for the identical chemical conditions of Case C-4.

7.0 FUTURE ENHANCEMENTS

The current implementation of the CAMEO code has focused on diffusive mass-transport modes for general corrosion of copper canisters under reducing and oxidizing conditions. Furthermore, the implementation has been structured in accordance with the specific objectives of SKI's SITE-94 project. Because of the emphasis on site characteristics and performance within SITE-94 analyses, commensurate emphasis was placed on including chemical environmental conditions into the corrosion models implemented in this initial version of CAMEO. Of particular interest to the SITE-94 project are plausible scenarios possibly leading to "early" failure of the copper canister.

There are a number of possible future enhancements and modifications that have been recognized during the development of CAMEO. While these items presented below are not exhaustive in scope, they are provided here as a basis for further discussions regarding the capabilities and use of the CAMEO code.

1. The current implementation of CAMEO assumes a reference Advanced Cold Process canister, with reference thickness of the outer copper vessel. It may be desirable to permit flexibility in assigning reference properties for the canister.
2. Impacts on chemistry at the canister surface arising from gamma radiation have not been considered. Especially if thinner canisters are to be evaluated, inclusion of a model to describe the potential impacts of gamma radiation may be desirable in future versions of CAMEO.
3. The bentonite buffer can chemically affect, if not control, the composition of pore water at the canister surface. It has also been suggested that migrating copper chloride species might react with minor Fe(II)-bearing phases in the buffer, such as pyrite or smectite. Other than adsorption, however, potential interactions between the buffer and pore water are not directly included in CAMEO at this time. Indirectly, the formation of copper iron sulphides in the buffer could be simulated if appropriate values for the solubility and degree of copper substitution in such a phase are specified. This would be akin to the modelling of mobile precipitation fronts as demonstrated with the CALIBRE code [28].
4. Pitting is currently handled by the user-assignment of pitting factors that adjust general corrosion rates for both reducing and oxidizing conditions. It might be possible to develop models for pitting that are conditioned on the composition (e.g., pH, Eh, chloride concentration) of pore water at the canister surface.
5. By analogy to calculation of radionuclide release (the original purpose and capability of the parent CALIBRE code), the inner concentration boundary condition for copper chloride at the canister surface can be controlled either by kinetic rate or diffusive mass-transport rate. In order to establish which is limiting and to evaluate the *chemical* (as compared to *physical*) effect of precipitation of corrosion products on long-term general corrosion rates, it was decided to include a separate kinetic rate model within CAMEO. A simple transition-state kinetic model has been incorporated into CAMEO, and a more detailed kinetic model could be added. It is not clear, however, if there is a need to incorporate additional kinetic constraints into CAMEO. Initial calculations reported here indicate that it is conservative to ignore such kinetic limitations.
6. Precipitation of Cu (II) compounds (e.g., CuO, $\text{CuCl}_2 \cdot 3\text{Cu}(\text{OH})_2$) away from the canister surface can be evaluated with the current implementation of CAMEO. Information (or a chemical model) for determining the solubility of such compounds is not included, however (see Point #3 above). An alternate rate law for Cu(I) oxidation to Cu(II) also could be considered. Results reported here, however, suggest that the oxidation of Cu(I) to Cu(II) has no measurable impact on the predicted rates of general corrosion for copper.
7. The impact of the emplacement tunnel is not addressed in this initial version of CAMEO. In CALIBRE, the effects of the tunnel on radionuclide releases may be studied in an approximate manner by including the bentonite and rock above the canister and setting the concentration at the upper boundary (defined by the interface of the buffer and rock with the tunnel) to zero. The effects of

the tunnel on the corrosion models in CAMEO would require more detailed examination and testing.

8. The potential impact on general corrosion of copper canisters from cycling of geochemical conditions in the near field (arising from variations in the far field) have not been evaluated in this report. Such an effort would first require development of revised conceptual models prior to modifications of CAMEO. Even after such modifications, it may only be possible to analyze such variations in an approximate manner with CAMEO.
9. Initial calculation of a fractured buffer confirms a profound, deleterious effect on general, uniform corrosion rate. Indeed, the thickness and coherence of the buffer are crucial factors in the demonstration of a robust, long-lived copper canister. If warranted from other analyses or scenario evaluations, the sensitivity of predicted failure by general corrosion arising from variation in these factors can be evaluated.

ACKNOWLEDGEMENTS

The authors wish to especially acknowledge the useful technical discussions with, and suggestions by, Frasier King of the Atomic Energy of Canada, Limited. Rolf Sjöblom provided the impetus behind this study, as well as extremely helpful comments on earlier drafts.

REFERENCES

1. KBS, (1983), *Final Storage of Spent Nuclear Fuel. KBS-3*. SKBF/KBS, Swedish Nuclear Fuel Supply Co., Stockholm, Sweden.
2. SKB (1992), *SKB-91, Final Disposal of Spent Nuclear Fuel. Importance of the Bedrock for Safety*. SKB Technical Report 92-20, Swedish Nuclear Fuel and Waste Management Co., Stockholm, Sweden.
3. SKI (1991), *SKI Project-90*, SKI Technical Report 91-23, Summary, Vols. I and II, August 1991, Swedish Nuclear Power Inspectorate, Stockholm, Sweden.
4. King, F. and D. LeNeveu, (1992), "Prediction of the lifetimes of copper nuclear waste containers, nuclear waste packaging," *Focus '91*, American Nuclear Society, LaGrange Park, IL, 1992) pp. 253-261.
5. King, F., D. M. LeNeveu and D. J. Jobe, (1993), "Modelling the effects of evolving redox conditions on the corrosion of copper containers," *Scientific Basis for Nuclear Waste Management XVII*, Materials Research Society, Pittsburgh, PA, pp. 901-908.
6. Worgan, K. and P. Robinson, (1993), *The CALIBRE Source Term Code: Technical Documentation for Version 2*, Intera Information Technologies Report No.: IM3583-3, Version 1, November 1993.
7. Worgan, K. and P. Robinson, (1993), *User Guide for CALIBRE*, Version

8. SKN, (1992), *Stability of Metallic Copper in the Near Surface Environment*, SKN Report 57, National Board for Spent Nuclear Fuel, Stockholm Sweden.
9. Garrels, R. M. and C. L. Christ, (1965), *Solutions, Minerals, and Equilibria*, Freeman, Copper & Company, San Francisco, CA, 450 p.
10. Lemire, R. J. and F. Garisto, (1989), *The Solubility of U, Np, Pu, Th and Tc in a Geological Disposal Vault for Used Nuclear Fuel*, Atomic Energy of Canada, Limited, Pinawa, Manitoba, Canada.
11. Barnes, H.L., (1979), "Solubilities of ore minerals", in *Geochemistry of Hydrothermal Deposits* (Ed. H. L. Barnes, Wiley-Interscience, New York, NY, pp. 404-460.
12. Giggenbach, W., (1974), "Equilibria involving polysulfide ions in aqueous sulfide solutions up to 240°C," *Inorg. Chem.*, 13, pp. 1724-1730.
13. Giggenbach, W., (1974), "Kinetics of the polysulfide-thiosulfate disproportionation up to 240°C," *Inorg. Chem.*, 13, pp. 1730-1733.
14. Wikberg, P., (1988), "The natural chemical background conditions in crystalline rocks," *Scientific Basis for Nuclear Waste Management XI*, Materials Research Society, Pittsburgh, PA, pp. 373-382.
15. Pedersen, K., S. Ekendahl, and J. Arlinger, (1991), *Microbes in Crystalline Bedrock. Assimilation of CO₂ and Introduced Organic Compounds by Bacterial Populations in Groundwater from Deep Crystalline Bedrock at Laxemar and Stripa*, SKB Technical Report 91-56, Swedish Nuclear Fuel and Waste Management Co., Stockholm, Sweden.
16. Fauque, G., Legall, J. and Barton L., (1991), "Sulphate-reducing and sulfur-reducing bacteria," in *Variations in Autotrophic Life* (Eds. J. Shively and L. Barton), Academic Press, London, pp. 271-337.
17. Neretnieks, I., (1986), *Chemical Geology*, 55, pg. 175.
18. Werme, L., P. Sellin and N. Kjellbert, (1992), *Copper Canisters for Nuclear High Level Waste Disposal: Corrosion Aspects*, SKB Technical Report 92-26, Swedish Nuclear Fuel and Waste Management Co., Stockholm, Sweden.
19. Werme, L., (1990), *Near-field Performance of the Advanced Cold Process Canister*, SKB Technical Report 90-31, Swedish Nuclear Fuel and Waste Management Co., Stockholm, Sweden.
20. Helgeson, H. C., J. M. Delany, H. W. Nesbitt, and D.K. Bird, (1979), "Summary and critique of the thermodynamic properties of rock-forming minerals," *Amer. J. Sci.*, 278A, 229 p.
21. Sharma, V. K. and F. J. Millero, (1988), *Environ. Sci. Tech.*, 22, pp. 768-771.
22. Lerman, A., (1979), *Geochemical Processes: Water and Sediment Environments*, John Wiley & Sons, New York, NY, 481 p.

23. Eary, L. E. and J. A. Schramke, (1990), "Rates of inorganic oxidation reactions involving dissolved oxygen," Chapter 30 in *Chemical Modelling of Aqueous Systems II*, American Chemical Society, New York, NY.
24. Shaw, W. and D. Worth, (1992), *Scoping Calculations for Canister-Tunnel Migration of Corrodants, Oxidants and Radionuclides*, SKI Technical Report 91:19, Version 2, 1992.
25. Carslaw, H. S. and J. C. Jaeger, (1959), *Conduction of Heat in Solids*, p. 296, Oxford Science Publications, Clarendon Press, Oxford, U.K.
26. Smellie, J. and M. Laaksoharju, (1992), *The Äspö Hard Rock Laboratory: Final Evaluation of the Hydrogeochemical Pre-Investigations in Relation to Existing Geologic and Hydraulic Conditions*, SKB Technical Report 92-31, Swedish Nuclear Fuel and Waste Management Co., Stockholm, Sweden, Table 6.3
27. Written communication from C. Lilja, SKI, dated 2 May 1994.
28. Worgan, K. and M. Apter, (1992), "The effect of precipitation fronts induced by radionuclide chain decay and elemental solubility limits on near-field mass transport," *Scientific Basis for Nuclear Waste Management XV*, Materials Research Society, Pittsburgh, PA, pp. 705-712.

SKi

STATENS KÄRNKRAFTINSPEKTION
Swedish Nuclear Power Inspectorate

Postadress/Postal address

SKI
S-106 58 STOCKHOLM

Telefon/Telephone

Nat 08-698 84 00
Int +46 8 698 84 00

Telefax

Nat 08-661 90 86
Int +46 8 661 90 86

Telex

11961 SWEATOM S